Journal of Drug Delivery Science and Technology 95 (2024) 105582

Contents lists available at ScienceDirect

Journal of Drug Delivery Science and Technology

journal homepage: www.elsevier.com/locate/jddst

Tailored binary polymer system PCL-PEO for advanced biomedical applications: Optimization, characterization and in vitro analysis

Ayda Afshar [a,*], Hamta Majd [a], Anthony Harker [b], Mohan Edirisinghe [a]

[a] Department of Mechanical Engineering, University College London, London, WC1E 7JE, UK
[b] Department of Physics and Astronomy, University College London, London, WC1E 6BT, UK

ARTICLE INFO

Keywords:
Polymer
Binary
Fiber
Drug delivery
Pressurized gyration

ABSTRACT

Combining a hydrophobic polymer such as polycaprolactone (PCL) with a hydrophilic polymer polyethylene oxide (PEO) in a binary polymer system can enable a range of novel applications in biomedical engineering by permitting exceptional therapeutic release, antimicrobial possibilities, and heterogeneous tissue engineering scaffolds. In this work, both PCL and PEO were dissolved in chloroform at 15 w/v % at six different ratios to prepare binary polymer solutions. The rheological properties of the singular and binary polymer solutions were measured, and fibers were spun using pressurized gyration. The fiber morphologies of the prepared materials were studied using scanning electron microscopy (SEM). By immersing samples in deionized water, binary polymeric fibers with varying swelling behaviors were developed and analyzed using optical microscopy. The results were used to identify an optimum PCL:PEO binary mixture in chloroform. Chemical compositions of singular/binary polymer composites loaded with ibuprofen (IBP) were characterized by Fourier-transform infrared spectroscopy (FTIR) and thermal analysis was examined using differential scanning calorimetry (DSC). *In vitro* studies on PEO–IBP exhibited an instant release rate of 90 % in 40 s, whereas PCL–IBP and PCL: PEO–IBP revealed a sustained release of 87–96 % in 72 h, respectively. The results were used to discuss the potential use of binary polymer systems in biomedical applications.

1. Introduction

Polymers have been used as biomaterials in the forms of fibers [1] and composite tissue engineering scaffolds [2] for a range of biomedical applications [3,4] such as drug delivery systems [5], tissue engineering [6] and wound healing [7,8], all of which can improve therapeutic efficacy by enhancing regeneration [9–15]. The physical characteristics of the polymers, such as composition and biodegradation, as well as polymer properties, including size, shape, and surface chemistry, all have a significant impact on their behavior in biological settings [16–18].

Polycaprolactone (PCL) is a synthetic biodegradable polymer that has gained significant attention in the biomedical industry, particularly in the field of drug delivery, sutures, and implantable devices [19–23]. Its compatibility with a variety of polymers, as well as its formability and low cost, make it an attractive material for tissue engineering [24]. The Food and Drug Administration (FDA) approval of PCL has been a significant factor attracting biomaterial researchers, which allows for safer use in humans [25,26]. However, the hydrophobic characteristic of PCL is not suitable for cell adhesion, migration, proliferation, and differentiation, limiting its application as a functional scaffold [27]. Due to PCL's hydrophobicity, its degradation kinetics are slower, potentially limiting its applications that require rapid degradation rates. PCL exhibits remarkable potential for blending with different polymers to achieve specific mechanical and degradation characteristics [28,29]. Polyethylene oxide (PEO) is a hydrophilic, biocompatible polymer that can be fabricated into a high strength material by obtaining oriented morphologies [30]. However, PEO possesses limitations such as rapid dissolubility, making it undesirable for controlled drug delivery applications. Several researchers have reported the combination of PEO with natural and synthetic polymers [31,32], thus PEO blends can be utilized to address the shortcomings of PCL.

Although polymeric drug carriers have demonstrated controlled release of hydrophilic and hydrophobic drugs over extensive periods [33], there is an increasing demand for polymeric materials with tailored characteristics that can be utilized as drug carriers to enhance drug bioavailability by reducing side effects, improving drug solubility, and reducing the required dosage frequency [34,35]. The process of

* Corresponding author.
E-mail address: ayda.afshar.18@ucl.ac.uk (A. Afshar).

https://doi.org/10.1016/j.jddst.2024.105582
Received 10 November 2023; Received in revised form 3 March 2024; Accepted 12 March 2024
Available online 13 March 2024

developing and synthesizing new polymers can be complicated and expensive [36]. As a result of homogenous integration, it would be beneficial to combine desired characteristics from respective materials into binary polymer systems and composites as an effective method for creating new materials with tailored physicochemical properties [37–40]. This approach can be used to compromise the hydrophobic nature of PCL by blending it with a hydrophilic PEO polymer that is designed to promote water migration to the proximal regions of PCL chains, thereby speeding up hydrolytic degradation [41–47]. While electrospun fibers made from PCL-PEO polymer blends have been extensively studied by Eskitoros-Togay et al. [48], and Darbasizadeh and co-workers [35], binary polymer systems have yet to be generated using cutting edge pressurized gyration (PG) with optimized properties.

In a previous publication [49], we reviewed binary polymer systems for biomedical applications and provided a comparison of PG with other production methods such as electrospinning and centrifugal spinning. PG is a relatively novel process that has gained popularity among associations pursuing large-scale manufacturing [49]. It is utilized in the single-step fabrication of fibrous materials and polymer blends that incorporate active pharmaceutical components. As opposed to electrospinning, which necessitates a high-voltage operation for fabrication [50], PG provides intriguing prospects by offering nozzle-free, cost-effective, mass production in rapid time, bypassing the high-voltage electric field required for fiber fabrication. PG offers ease of production, adjustable processing parameters, and controllable fiber morphology to satisfy function, topography, size, and scale-up requirements, making it an effective approach for mass production of low micro-nano diameter fibers, particular for drug delivery systems. Expanding on this approach, this study introduces a novel pressure spun blend system that uses a scalable approach with optimum working parameters to obtain an optimized PCL:PEO polymer ratio to present a novel binary class of material with improved properties for advanced biomedical engineering applications. The optimized biomaterial was incorporated with ibuprofen (IBP), resulting in enhanced rate of drug release that alleviated the limitations of singular polymers. Fiber composites were compared on the basis of their morphology, physical properties, swelling behavior, chemical compositions, and drug release profiles.

2. Experimental details

2.1. Materials

Polycaprolactone (PCL, M_W 80 000 $gmol^{-1}$), polyethylene oxide (PEO, M_W 200 000 $gmol^{-1}$), ibuprofen (IBP, M_W 206.28 $gmol^{-1}$) and chloroform (Chl, CAS Number: 67–66–3) were purchased from Sigma Aldrich, UK. Phosphate buffer saline (PBS, pH = 7.4) was purchased from Oxoid ThermoFischer, UK.

2.2. Polymer solutions

Primary 15 w/v % PCL and 15 w/v % PEO solutions were prepared using Chl. Subsequently, six different binary PCL:PEO polymer solutions were created at increasing PEO ratios (1 w/v % (14:1), 3 w/v % (4:1), 5 w/v % (2:1), 7 w/v % (8:7), 9 w/v % (2:3), and 11 w/v % (1:4)). The singular polymer solutions and optimized PCL:PEO binary polymer formulations were then incorporated with 4 wt % IBP. All polymer solutions were mixed under ambient conditions (20–23 °C) with relative humidity (40–50 %) and stirred for 24 h using a magnetic stirrer.

2.3. Binary fiber composite

Spinning was carried out using pressurized gyration (Fig. 1). The setup consists of an aluminum cylindrical vessel containing the polymer solution, measuring 60 mm in diameter with 24 orifices through the wall, each measuring 0.5 mm. The vessel was connected to nitrogen gas supply, allowing applied pressures ranging of 0.1–0.3 MPa. The vessel was subjected to a constant rotational speed of 10 000 rpm and applied pressure of 0.1 MPa. All experiments were conducted for 15 s by inserting 2 mL polymer solution in the vessel at a temperature of 20–23 °C, with relative humidity ranging from 40 to 50 %.

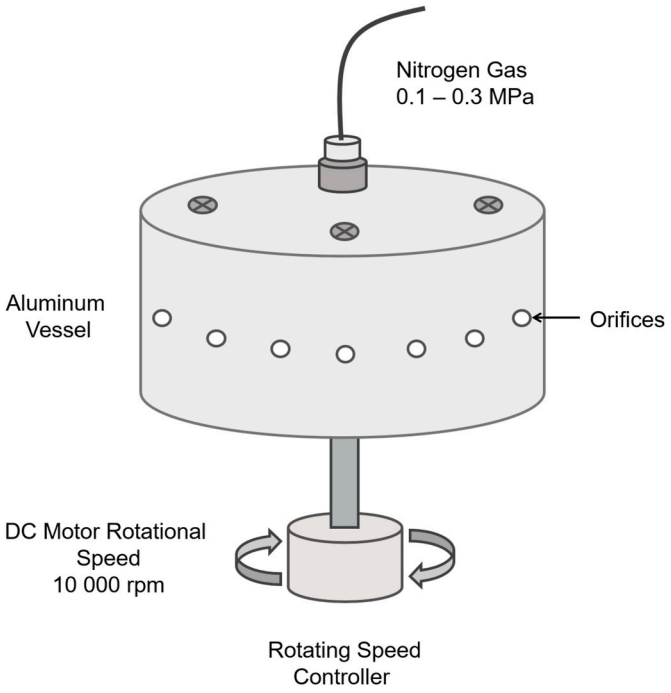

Fig. 1. Schematic illustration of binary composite production using pressurized gyration.

2.4. Characterization

2.4.1. Rheology

Viscosity of the polymer solutions was measured using a calibrated programmable rheometer (DV-III Ultra, Brookfield Engineering Laboratories INC, Massachusetts, USA) with shear rate values ranging between 0.04 and 1.77 s^{-1}, and shear stress values in the range 0.38–7.34 Pa. For each sample, 14 different measurements were taken, and each test was repeated three times.

The power law equation was used to define polymer solution behavior, described in Eq. (1) [51], where σ is the shear stress, K is the constant, $\dot{\gamma}$ is the shear rate, and n is the flow index of the fluid, which ranges from $0-1$. For $n = 1$, the behavior is Newtonian, $n < 1$, the fluid is non-Newtonian, known as a pseudoplastic fluid/shear thinning, and if $n > 1$, the fluid is non-Newtonian, or dilatant fluid/shear thickening.

$$\sigma = K\dot{\gamma}^n \tag{1}$$

Flow behavior index, n is:

$$n = log_{10}\left(\frac{\sigma}{K}\right) \Big/ log_{10}(\dot{\gamma}) \tag{2}$$

2.4.2. Surface tension

The Wilhelmy's plate method was used to determine the surface tension of the solutions using a calibrated digital tensiometer (Tensiometer K9, Kruss GmbH, Hamburg, Germany). Each test was repeated five times at ambient temperature of 20–23 °C and a relative humidity of 40–50 %.

2.4.3. In vitro swelling

Six PCL:PEO binary fiber composites with varying PEO ratios (14:1–1:4) were used to investigate the effect of increasing PEO content

on swelling and morphological behavior of the fibers. Dry binary fiber samples were cut at ~50 mm and immersed in 0.3 mL deionized water within a Petri dish at 15 min intervals, ranging from 15 to 60 min. This procedure was repeated for all binary composites under ambient conditions, with a temperature of 20–23 °C and relative humidity of 40–50 %. Subsequently, all binary fiber composites were examined using an optical microscopy.

2.4.4. Optical microscopy

All swelling micrographs were captured using an optical microscope (KEYENCE Digital Microscope VHX-7000). The microscope was calibrated using a standard microscope slide and all samples were placed on a Petri dish (containing fibers immersed in deionized water) and positioned on the motorized eucentric stage. The microscope featured a high-resolution lens at 4K CMOS image sensor. Using the fully integrated head consisting of the 4-piece motorized revolver, images were observed utilizing the focus view camera and captured at 20–400 X magnifications. Images were taken at 15 min intervals for different binary PCL: PEO polymer compositions.

2.4.5. Scanning electron microscopy (SEM)

The morphology of PEO, PCL, and all binary PCL:PEO as well as IBP-loaded fibers were examined using scanning electron microscopy (GeminiSEM 360, Carl Zeiss Microscopy GmbH, Oberkochen, Germany) with 1–10 kV acceleration voltage. The fiber diameters were measured using computer-aided image visualization software (ImageJ 1.52a, National Institutes of Health, USA). The average and standard deviation values of the acquired results were statistically projected for each sample, and frequency graphs of fiber diameters were generated using statistics software (OriginPro 2021b, OriginLab Corporation). Utilizing the acquired information, a comparison was made between different singular/binary polymer formulations.

2.4.6. Fourier-transform infrared spectroscopy (FTIR)

After fiber production, FTIR spectroscopy (Thermo Fisher Scientific, Nicolet iS50 FTIR) was performed to confirm the implementation of binary polymers and integrated IBP. Prior to the measurements, 2 mg of PEO, PCL, optimized PCL:PEO, and drug loaded composites including IBP, PEO-IBP, PCL-IBP, and optimized PCL:PEO-IBP was positioned on the ATR crystal and studied over 10 rounds in the range of 4000–1000 cm^{-1} at a resolution of 4 cm^{-1} to record the measurements.

2.4.7. Differential scanning calorimetry (DSC)

The change in physical properties of PEO–IBP, PCL–IBP, and optimized PCL:PEO–IBP fiber composites were determined by using DSC 3 Mettler Toledo device, Mettler Toledo instrument and STAR^e software. Prior to the measurements, 5 mg of each sample was positioned in aluminum DSC pans, hermetically sealed, and heated from 0 to 300 °C at a rate of 10 °C/min under a 50 mL/min gas flow (N_2).

2.4.8. Loading of ibuprofen and in vitro release studies

2.4.8.1. IBP encapsulation efficiency. The encapsulation efficiency (EE) of IBP content in the composites was determined by dissolving 20 mg of PEO-IBP, PCL-IBP and optimized PCL:PEO-IBP in 20 mL of chloroform. The samples were stirred at 2000 rpm for 8 h to completely dissolve the IBP from the composites into the solvent. Subsequently, 2 mL of the filtered solution's absorbance was measured at 267 nm using a UV JENWAY 7315 spectrophotometer. The EE of IBP was calculated using Eq. (3) [52].

$$EE\ (\%) = \frac{Mass\ of\ IBP\ content\ in\ composites\ (mg)}{Theoretical\ total\ mass\ of\ IBP\ (mg)} \times 100\ \% \tag{3}$$

2.4.8.2. Disintegration. Disintegration of PEO-IBP composites was carried out in 20 mL PBS at 37 °C. Prior to testing, a rectangular section of 200 mm diameter was cut from the composites and immersed in a Petri dish. A Canon EOS 1000D video camera was used to capture the disintegration and soaking of the composites at 60 frames per second.

2.4.8.3. Dissolution. The dissolution test was conducted to analyze the release kinetics of PEO-IBP, PCL-IBP and optimized PCL:PEO-IBP. Prior to the release experiment, a linear calibration curve was created using a series of standard solutions with concentrations ranging from 0.003 to 0.3 mg/mL. For the release study, 20 mg from each composite was immersed into a 20 mL test medium and incubated in a shaker at 37 °C. Moreover, for PEO–IBP, samples were collected at predetermined intervals of 5, 10, 20, 30, and 40 s, given the hydrophilic nature of the composites. However, for PCL–IBP and PCL:PEO–IBP, samples were taken at 2, 4, 6, 8, 24, 48, and 72 h. In each case, 2 mL of supernatant from the assessment medium was removed and replaced with 2 mL of new test medium to maintain a sink condition. The removed supernatant was filtered using a 0.22 μm Millipore and analyzed using a UV spectrophotometer. The obtained data collected were used to calculate the cumulative release percentage using Eq. (6) [52]. All experiments were carried out in triplicate.

$$IBP\ release\ (\%) = \frac{A_t\ (mg)}{A_s\ (mg)} \times 100\ \% \tag{4}$$

Where, A_t is the amount of IBP released at time t and A_s is the maximum amount of IBP released.

2.4.9. Mathematical modelling

Two mathematical models were used to describe the release of ibuprofen from the fibers into solution. The first model assumes a simple dissolution, as described by Noyes and Whitney [53]. If the rate of dissolution (mass M per unit time t) from a surface area S is

$$\frac{dM}{dt} = \alpha S \tag{5}$$

then for a cylindrical fiber of initial radius r_0 and density ρ, the fractional dissolution is

$$\varphi_{NWc}\ (t) = 2t \Big/ \tau - (t/\tau)^2 \tag{6}$$

where the timescale $\tau = r_0\ \rho / a$.

The other release model assumes that ibuprofen undergoes Fickian diffusion through the fiber, with free dissolution at the surface of the fiber. This is a standard problem in diffusion, and a good fit to the exact analytic release rate is given by

$$\varphi_{FC}(t) = \varphi_{max}\ \tanh\ (2.415\sqrt{(t\ /\ \tau)}), \tag{7}$$

where φ_{max} is the maximum fractional release and in this case the timescale is related to the fiber radius r_0 and the diffusion coefficient D of the drug in the polymer matrix, $\tau = r_0^2/D$. This expression has been derived by adapting the methods of the appendix of a previous paper from spherical particles to cylindrical fibers [54]. This form has advantages over the Korsmeyer-Peppas expression, which is commonly used, as it can be applied over the whole range of the release from 0 to 100 % and the fitting parameters can be related to the diffusion coefficient of the drug.

3. Results and discussion

3.1. Physical properties

The fundamental properties of the PG spinning mixture, including molecular weight, solution concentration, viscosity and surface tension possess a substantial impact on polymer solution spinnability, fiber morphology and topography [55]. Among these factors, viscosity and surface tension have the most significant effect in the spinning system.

The physical chain interlocking of the polymers increases as the solution viscosity and concentration increase. This interlocking of polymer chains functions similarly to chemical cross-links and serves an important purpose in stabilizing the polymer jet, which, along with solvent evaporation, controls the procedures of fiber development in PG [56]. The entanglement of polymer chain restricts jet formation [57], and within a specific viscosity range, as the viscosity of the polymer mixture increases up to a critical value, the fiber diameter increases, as does the relative time required for the elongation of the polymer jet, due to the incremental amounts of physical entanglement between polymer chains. When the solution viscosity is excessively high, centrifugal force cannot overcome surface tension [55]. Even so, post-stretching, the polymer jet can retain a specific shape and eventually form uniform bead-free fibers [58,59]. However, if the viscosity is below the critical value, fibers with bead-on-string structure will develop. Furthermore, as the solvent (chloroform) evaporates from the polymer jet, the temperature at the air-liquid interface will decrease rapidly due to the enthalpy of vaporization [55]. However, there have been insufficient studies on complete chloroform separation, which poses a potential limitation.

The viscosity (Fig. 2) and surface tension (Fig. 3) values varied based on the ratio of the binary PCL:PEO polymer solutions. In Table 1, the surface tension values range between 23.2 ± 1.2 mN m^{-1} to 44.0 ± 2.2 mN m^{-1}, respectively. The viscosity of PEO and PCL were 992 ± 10 mPa s and 325 ± 5 mPa s, while the surface tension was 43.8 ± 2.2 mN m^{-1} and 26.2 ± 1.3 mN m^{-1}, respectively. However, upon incorporating and increasing the PEO ratio in the binary polymer system, the viscosity of the mixtures increased from 337 ± 17 mPa s to 984 ± 49 mPa s, and the viscosity reduced to 793 ± 40 mPa s as the shear rate increased due to non-Newtonian shear thinning effects. The findings suggest that PEO exhibits a higher viscosity and surface tension than PCL. Although the total polymer concentration was kept at 15 w/v %, when compared to individual polymer mixtures, the broad data for the binary polymer solutions can be attributed to an increased PEO ratio in PCL. The increase in the polymer solution properties is associated with polymer chain entanglement. Hence, a higher viscosity and surface tension can be an indication of greater polymer entanglement provided by a high PEO ratio [60].

Fig. 2 shows that at higher shear rates, the viscosity was near stability, whereas at lower shear rates, there was a greater fluctuation. A flexible and flowing polymer solution can cause the molecules to stretch and deform in the flow direction. The slower the molecules recover to their original shapes, relative to the rate of shear, the more they align with the flow. Aligned molecules contribute less to the polymer solution viscosity. In steady shear conditions, the solution viscosity was highest when the shear rate was low, indicating that molecules can realign and relax to their undisturbed configuration promptly as they move. However, as shear rate increases, the molecules cannot separate as quickly, therefore viscosity decreases [61,62].

For all cases in Fig. 2, the relationship of shear stress increased with shear rate which satisfied the power law. The flow index behavior (n), gives the flow properties of all polymer solutions, displayed in Table 1.

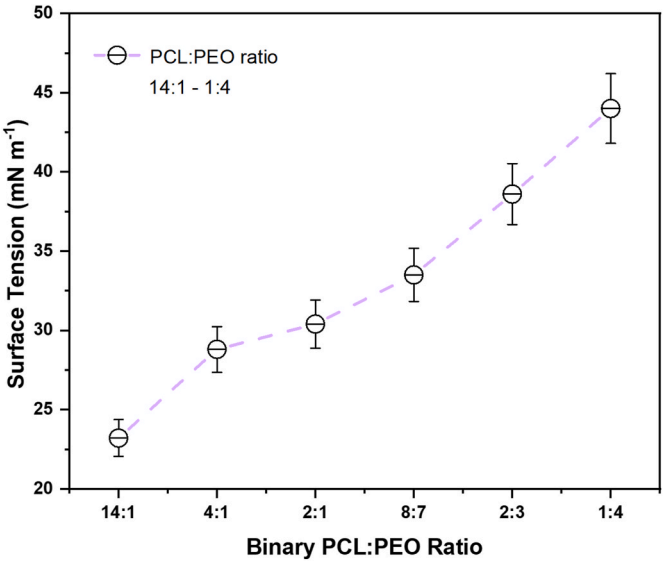

Fig. 3. Relationship between surface tension and increase in PEO ratio of PCL: PEO binary polymer systems.

Table 1
Polymer solution properties for singular and binary PCL:PEO compositions.

Polymer Solution, PCL: PEO (w/v %)	Surface Tension (mN m^{-1})	Viscosity (mPa s)	Flow Behavior Index, *n*
PEO 100	43.8 ± 2.2	992 ± 10	0.92
PCL 100	26.2 ± 1.3	325 ± 5	0.66
14:1	23.2 ± 1.2	346 ± 17	1.9
4:1	28.8 ± 1.4	337 ± 17	1.3
2:1	30.4 ± 1.5	463 ± 23	0.97
8:7	33.5 ± 1.7	490 ± 25	0.88
2:3	38.6 ± 1.9	984 ± 49	1.05
1:4	44.0 ± 2.2	793 ± 40	0.96

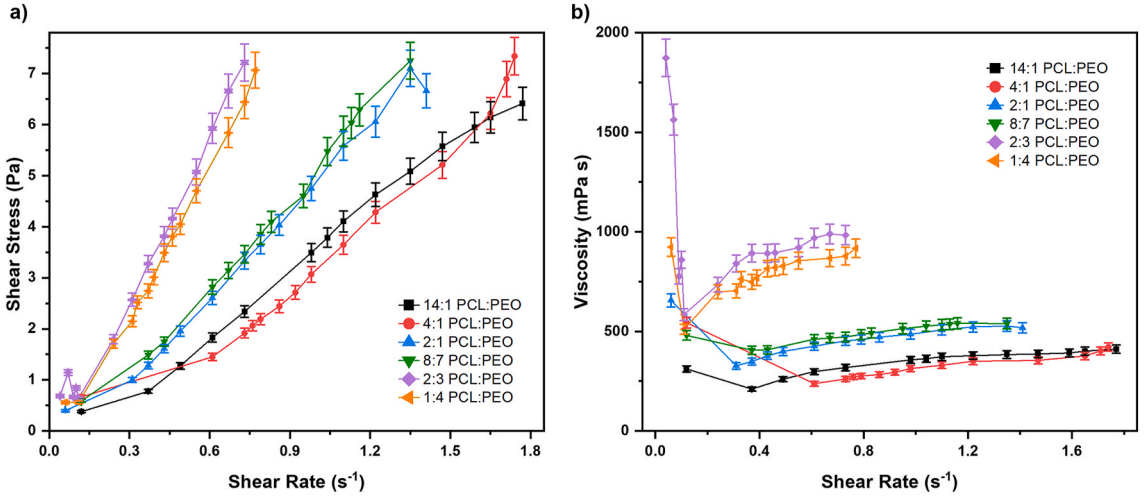

Fig. 2. Graphs showing a) shear rate vs shear stress for the PCL:PEO binary polymer system at ratios 14:1–1:4, and b) viscosity vs shear rate for the PCL:PEO binary polymer system at ratios 14:1–1:4.

PCL and PEO polymer mixtures exhibit n values between 0.66 and 0.92, and binary polymer solutions reveal n values ranging between 0.88 and 1.3, suggesting non-Newtonian fluid flow behavior, where n values < 1 indicate pseudoplastic fluid behavior or shear thinning. Whereas PCL: PEO in the ratios 14:1, 4:1 and 2:3 demonstrate a dilatant fluid behavior with n values ranging between 1.05 and 1.9, corresponding to shear thickening behavior.

3.2. Fiber morphology

In this study, polydispersity index (PDI) is used as a representation to describe the degree of non-uniformity of all fiber composite size distributions. PDI ranges from 0 to 1.0, where 0 is a perfectly monodisperse sample, and 1.0 is a highly polydisperse sample [63,64]. In drug delivery applications, samples with PDI values of 0.3 and below are considered acceptable and indicate a homogenous population [65]. However, samples with PDI values greater than 0.7 indicate a broad size distribution which is undesired.

For optimal fiber yield and morphology, 0.1 MPa gas pressure was applied after reaching critical rotational speed of 10 000 rpm. Fig. 4 (a-b) shows SEM micrographs of 15 w/v % PEO and PCL composites dissolved in Chl, respectively. The resulting fibers were analyzed for their morphologies owing to differences in the use of polymers. PEO fibers in Fig. 4 (a) showcase a continuous, smooth surface and almost aligned orientation, although some entanglement was observed. Average fiber diameter of PEO was 1.9 μm with a PDI of 47 %. PCL fibers demonstrate an average diameter of 3.7 μm, PDI 35 %, and an average bead diameter of 35.9 μm, PDI of 33 %, revealing random fiber orientation. The individual polymers present a monodisperse distribution.

PEO possessed higher viscosity, indicating that the spinning fluid can be stretched into fine jets, as suggested earlier in Table 1. PEO's high molecular weight determines that the solution concentration meets the critical value, which corresponds to sufficient chain entanglement to form continuous spinning jets, resulting in smaller fiber diameters. However, PCL polymer solution demonstrated a lower viscosity, surface tension, and molecular weight, resulting in bead-on-string formation with a larger fiber diameter due to reduced chain entanglement. With an increase in the PEO ratio, the product of PG under the same working parameters gradually changes from bead-on-string fibers to smooth bead-free fibers [66].

SEM micrographs in Fig. 4 (c-h) were deployed to characterize the binary polymer composites (14:1–1:4). At the lowest PEO ratio of 14:1 in PCL:PEO, fibers were observed with high bead frequency, demonstrating an average diameter of 31.1 μm, PDI of 41 %, and an average fiber diameter of 3.4 μm with a PDI of 53 % (Fig. 4 (c)), suggesting a polydisperse distribution. The PCL:PEO binary composites with higher PCL ratios retained their bead-on-string morphology, attributing to PCL's low surface tension of 26.2 ± 1.3 mN m^{-1} (Table 1), which can result in irregular ejection of the polymer solution since the polymer can easily escape vessel orifices even at slower rotational speeds [67]. With an increase in the PEO ratio, there is a reduced occurrence of beaded fibers. Furthermore, aligned porous fibers with an average pore diameter of 0.07 ± 0.04 μm was observed in PCL:PEO 4:1 followed by an average fiber diameter of 2.8 μm, PDI 29 % (Fig. 4 (d)), suggesting a monomodal distribution. Micropores with a diameter of 1–10 μm promote cell adhesion and facilitate nutrient absorption [68]. In Fig. 4 (e–f) at 2:1 and 8:7 PCL:PEO compositions, similar observations to Fig. 4 (c) were detected, revealing an average bead diameter of 34.7 μm, PDI of 58 %, 30.8 μm PDI of 42 %, and average fiber diameters of 2.7 μm and 2.6 μm, indicative of PDI of 44 % and 31 %, respectively. At 2:3 PCL:PEO composition, the average fiber diameter was 1.8 μm, PDI of 28 % (Fig. 4 (g)). At 1:4 PCL:PEO binary ratio, the average fiber diameter was at its lowest range of 1.5 μm with a PDI of 27 % (Fig. 4 (h)). When increasing the PEO ratio, a PDI of 53–27 % was obtained, corresponding to a monomodal distribution. This finding shows that the generated composites and distributions can be tailored and controlled using the binary polymer system. Similarly, Mirzaei et al. [28] reported fibrous scaffolds manufactured through the electrospinning of PEO:PCL blends dissolved

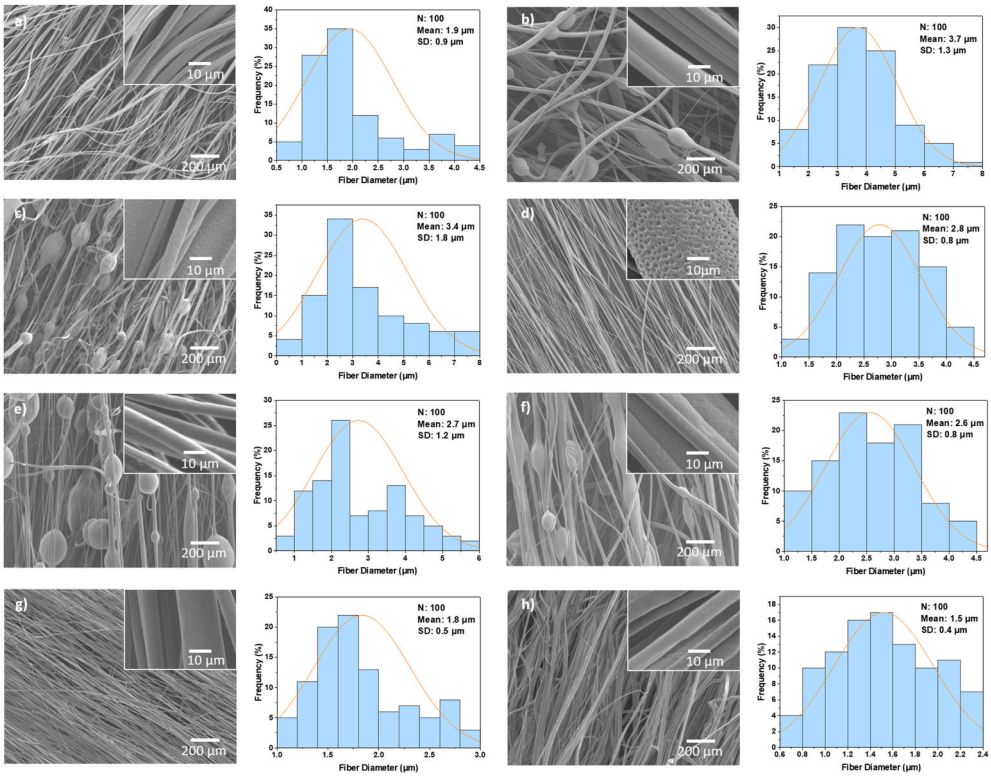

Fig. 4. SEM micrographs of: a) 15 w/v % PEO, b) 15 w/v % PCL, c) PCL:PEO 14:1, d) PCL:PEO 4:1, e) PCL:PEO 2:1, f) PCL:PEO 8:7, g) PCL:PEO 2:3 and h) PCL:PEO 1:4, respective fiber diameter distributions all spun at 10 000 rpm, 0.1 MPa applied pressure.

in chloroform. It was demonstrated that the amount of PEO influenced hydrophilicity, biodegradability, and mechanical properties. The fiber diameters ranged from 0.9 ± 0.1 μm–1.6 ± 0.1 μm for PEO:PCL/30:70 – PEO:PCL/50:50, respectively [28]. In this study, the addition of PEO to PCL rendered the binary composites from hydrophobic to hydrophilic.

Considering the PDI values, majority of the fiber composites exhibited pronounced polydispersity. Fibers with diverse size scales may be appropriate for a variety of applications. Nonetheless, the fibers generated in this study fall in the micrometer range, making it feasible to load and deliver small molecule drugs and components, that have the potential to deliver therapeutic elements [69].

It is further confirmed by Fig. 5 that as the PEO ratio of PCL:PEO increases, the average fiber diameters decrease from 3.4 to 1.5 μm. This may be associated to PEO's high molecular weight, which results in increased viscosity and polymer chain entanglement [70,71]. Surface tension must be within an optimum range, otherwise beads will occur. In this study, surface tension was overcome by chain entanglements, resulting in smaller fiber diameters.

3.3. Effects of swelling on binary fiber composites

A swelling test was performed to determine the effect of increased PEO ratio on fiber composite behavior when immersed in deionized water for 15–60 min of incubation. The average fiber diameter before and after immersion was measured to determine the degree of swelling. Fig. 6 displays the swelling behaviors of all binary polymer composites at various PEO ratios. The average fiber diameters range between 2.7 and 8.0 μm as shown in the optical micrographs in Fig. 7. In comparison to the SEM results of dry binary fiber samples in Fig. 4, it can be seen that after 15 min immersion in deionized water, PCL:PEO 14:1 possess a decreased average fiber diameter of 2.7 μm, PDI of 19 % (Fig. 7 (a)). However, at 30 min, it exhibits the highest swelling of 7.7 μm, PDI of 26 % (Fig. 7 (b)). Between 45 and 60 min, the average fiber diameters decreased to 7.6 and 7.3 μm, with PDI of 32 % and 29 %, respectively (Fig. 7 (c–d)). However, the swelling remained significant in comparison to 15 min. At 4:1 PCL:PEO, it was observed that the binary fibers revealed highest swelling of 4.7 μm, PDI of 40 % in the initial 15 min, followed by dilation of 4.0–2.8 μm, PDI of 33–32 % at 30–60 min, respectively (Fig. 7 (e–h)). At PCL:PEO ratio of 2:1, maximal swelling was detected at 30 min, with an average swelled-binary fiber diameter of 6.1 μm, PDI of 31 % (Fig. 7 (j)). However, during 45–60 min, binary composites indicate a consistent dilation of 3.2 μm, PDI of 25 % (Fig. 7 (k–l)). When compared to dry binary fibers of the same ratio, an overall swelling was detected between 15 and 60 min. During 15–30 min for 8:7 PCL:PEO, it was observed that the swelling remained constant at 3.6 μm, with PDI of 25–36 % (Fig. 7 (m–n)). At 45 min, the binary composites confirm highest swelling with an average diameter of 5.8 μm, PDI of 31 % (Fig. 7 (o)). The binary fibers dilate to 4.6 μm, PDI of 28 % (Fig. 7 (p)) at 60 min. In comparison to 14:1 PCL:PEO formulation, with increasing PEO in the binary polymer system 4:1, 2:1 and 8:7, the composites revealed a higher fiber diameter at 15 min incubation than at 60 min incubation (Fig. 6), resulting in an initial higher water content absorption in the fiber composites. This may be attributed to the increased PEO ratio in the blend mixtures, suggesting that water molecules entered the fibers at a faster rate when immersed in deionized water, allowing the binary fibers to swell significantly rapidly during the initial 15 min. However, during the remaining incubation phases, the hydrogen bonds restricted the migration of water molecules, which may have slowed down the swelling of fibers, and preventing them from swelling as much at 60 min. Whilst dry 2:3 PCL:PEO binary fibers expressed thinner diameters of 1.8 μm, PDI 28 %, when immersed in deionized water, the composites expose continuous swelling between 15 and 60 min, ranging at 5.2–7.2 μm, PDI of 25–29 % (Fig. 7 (q–t)). Similar observations were detected in PCL:PEO 1:4 with maximal swelling of 6.0–8.0 μm, PDI 23–33 % (Fig. 7 (u–x)). All binary samples demonstrate a monomodal

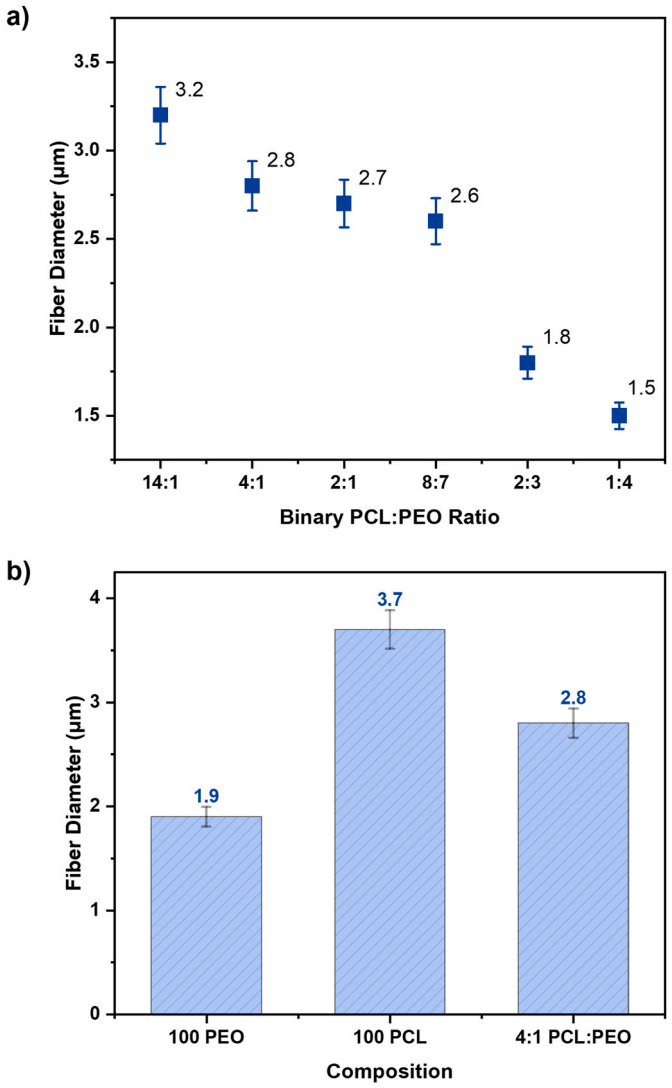

Fig. 5. a) The effect on average fiber diameter by increasing the PEO ratio in the PCL:PEO (14:1-1:4) binary system and b) average fiber diameter of PEO, PCL, and optimized PCL:PEO composites.

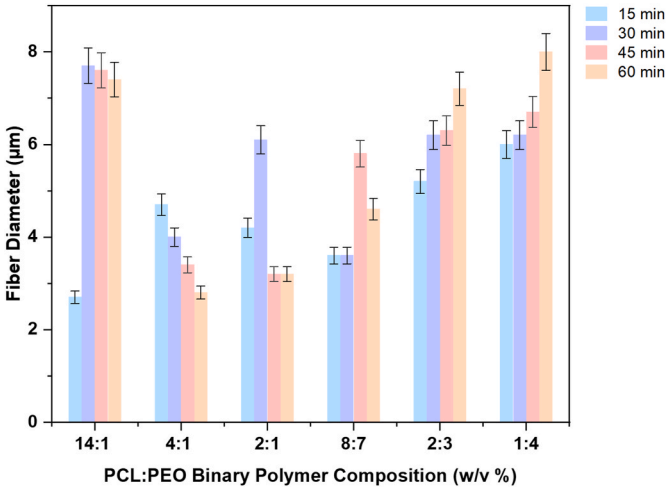

Fig. 6. Influence of increasing PEO ratio and swelling behavior on average fiber diameter using PCL:PEO binary polymer system at 14:1–1:4, immersed in deionized water for 15–60 min.

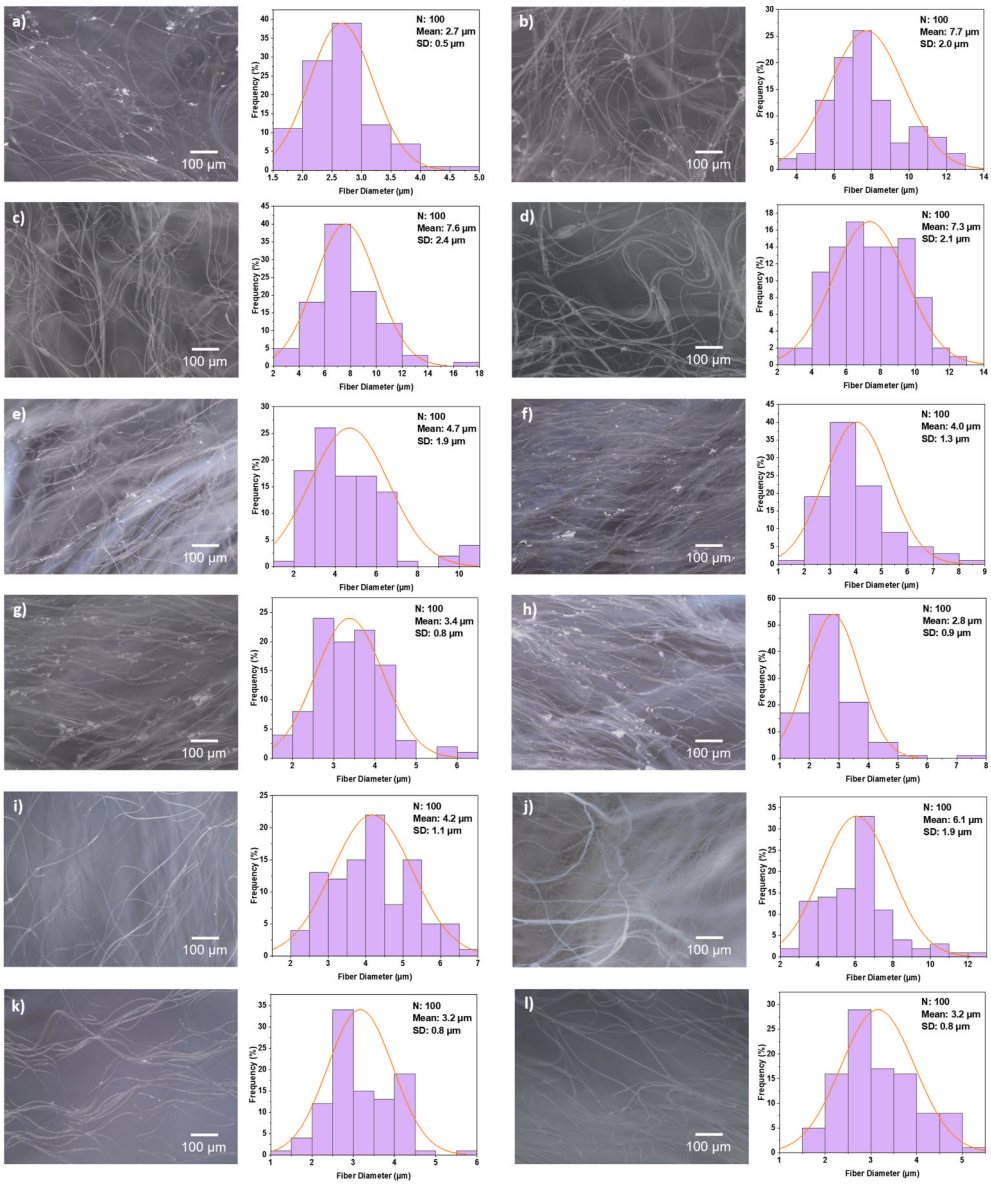

Fig. 7. Wet sampling optical micrographs of PCL:PEO binary polymer systems soaked in 0.3 mL deionized water for 15–60 min. Binary PCL:PEO ratios: a) 14:1 15 min, b) 14:1 30 min, c) 14:1 45 min, d) 14:1 60 min, e) 4:1 15 min, f) 4:1 30 min, g) 4:1 45 min, h) 4:1 60 min, i) 2:1 15 min, j) 2:1 30 min, k) 2:1 45 min, l) 2:1 60 min, m) 8:7 15 min, n) 8:7 30 min, o) 8:7 45 min, p) 8:7 60 min, q) 2:3 15 min, r) 2:3 30 min, s) 2:3 45 min, t) 2:3 60 min, u) 1:4 15 min, v) 1:4 30 min, w) 1:4 45 min, and x) 1:4 60 min, respective fiber diameter distributions all spun at 10 000 rpm, 0.1 MPa applied pressure.

distribution.

Maximal swelling behavior was achieved with a higher PEO ratio due to increased polymer chain entanglement (PEO $M_W = 200,000\ gmol^{-1}$). This is because PEO expands and swells when submerged in water, causing a significant enlargement. According to the results, PEO ratio and swelling duration both influence the properties of the binary polymer composites. Maximum osmotic pressure developed when fibers were immersed in deionized water, resulting in significant swelling. The presence of hydrophilic moieties in the polymeric structure of fibers results from their ability to absorb water and swell. When the rate of drug diffusion is faster than the rate of polymer swelling, swelling-controlled drug release occurs. For drug delivery systems, the rate and capacity of fiber water absorption, as well as the thickness of the composites, are crucial factors; hence, the higher the rate of swelling, the faster the drug release. PEO demonstrated superior swelling properties when combined with PCL. Thus, modifying the binary polymer ratio and the amount of PEO integrated in polymer preparation can enhance the water absorption and swelling ability of these fiber composites. PEO becomes hydrated and swollen when in contact with aqueous environments, forming a layer of hydrogel that controls the subsequent entry of water and dissolution of any active substance present in the polymer matrix [72]. As a result, increasing the PEO ratio allows for more water absorption and swelling. The decrease in physical crosslink density, which prevents the expansion of the amorphous regions, can be used to justify the sharp rise in water absorption with higher PEO concentrations [73]. The findings suggest that polymer swelling in aqueous environments can be regulated by optimized binary polymer systems. Furthermore, the polymer properties play a significant role in the diffusion of drugs into and out of the polymer matrix, and hence affects the release kinetics of the integrated drugs [74].

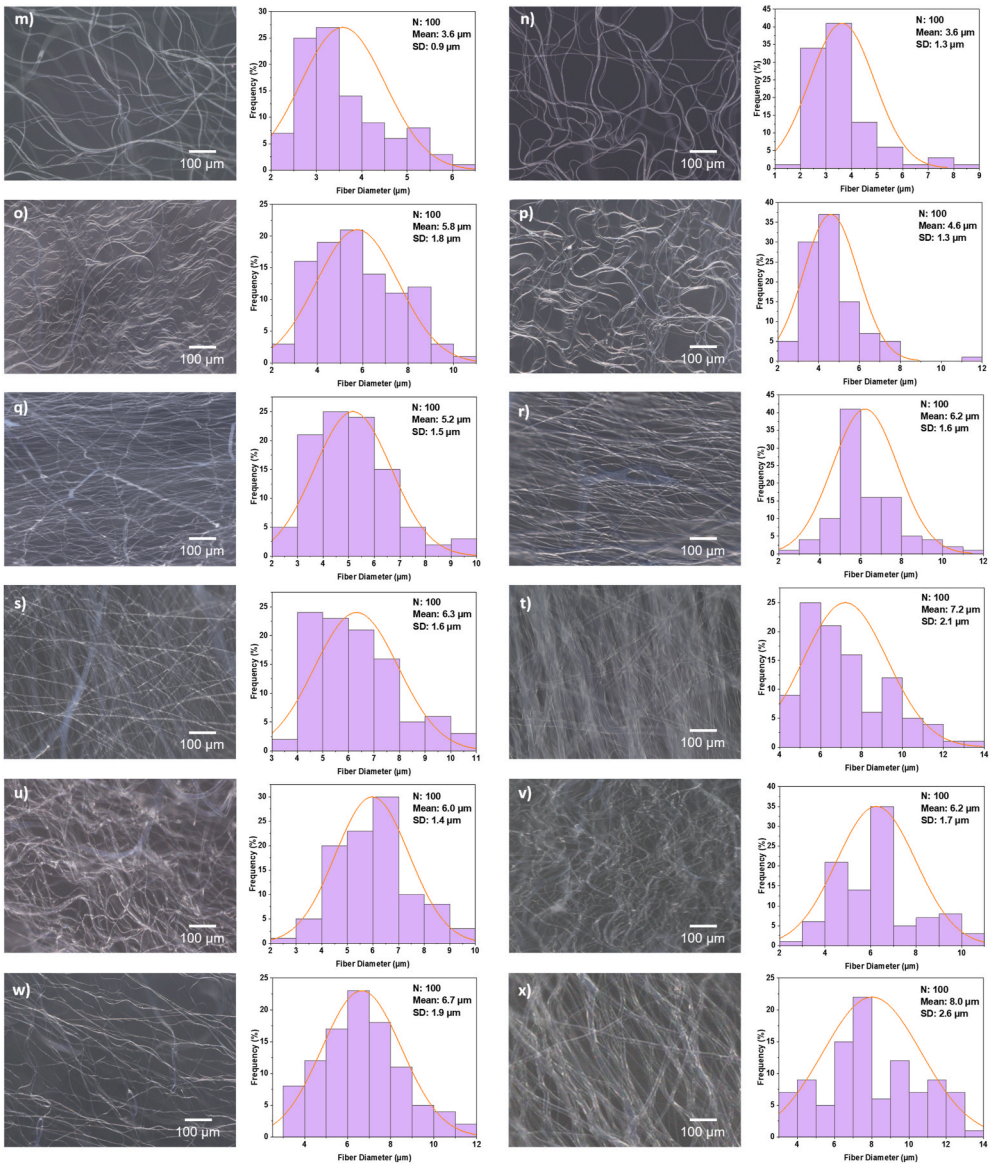

Fig. 7. (*continued*).

3.4. Optimized binary polymer system

After evaluating the physical properties of all polymer solutions, morphologies, and swelling capabilities, PCL:PEO 4:1 (3 w/v % PEO in 12 w/v % PCL) (Fig. 5 (b)) was determined as the optimal binary polymer formulation. PEO is known to possess a hydrophilic nature due to the presence of hydrophilic functional groups in the structure. Therefore, upon blending PEO with a hydrophobic polymer like PCL, a significant increase in the hydrophilicity of the blends took place in formulations 2:1, 8:7, 2:3. 1:4, and an increased swelling behavior resulted. Also, the increase in PEO ratio in the PCL:PEO compositions decreased the hydrophobicity of the resulting binary fiber composites. One goal of this research was to develop a binary polymer system with balanced hydrophobic and hydrophilic properties. Binary 4:1 PCL:PEO formulation delivered consistent swelling behavior with desired rheology beyond the range that can be obtained from singular polymer systems and binary formulations with increased PEO ratio. Binary composites with higher PCL ratios (14:1) were anticipated to possess hydrophobic characteristics like PCL, while composites with higher PEO ratios (2:3, 1:4) were likely to exhibit hydrophilic properties like PEO. Although formulations with a higher PEO ratio demonstrated smaller fiber diameters, offering a larger surface area to volume ratio, they would possess rapid drug release kinetics [75] which is undesirable for applications that require controlled/sustained drug release. As a result, determining the optimal ratio was critical for enabling the appropriate amount of hydrophilicity, suitable for biomedical applications.

3.5. Effect of ibuprofen

Rheological testing was performed for the optimal binary polymer formulation incorporated with IBP. The surface tension did not differ significantly, ranging at 27.3 ± 1.3 mN m^{-1}, however the viscosity was 256.5 ± 40 mPa s, with n value of 1.0. While both virgin and IBP-loaded polymer mixtures suggest a non-Newtonian shear thickening flow, the viscosity of the virgin optimal solution was higher (337 ± 17 mN m^{-1}). Nonetheless, critical justifications for the influence of IBP on rheological properties cannot be made since IBP integration was at a low concentration of 4 wt %.

SEM micrographs of PEO-IBP composites (Fig. 8 (a)) reveal continuous fibers, with an average diameter of 1.6 μm and a PDI of 38 %. In contrast, the PCL-IBP composites (Fig. 8 (b)) showed a larger average diameter of 3.2 μm, and a PDI of 31 %. Non-beaded fiber formation

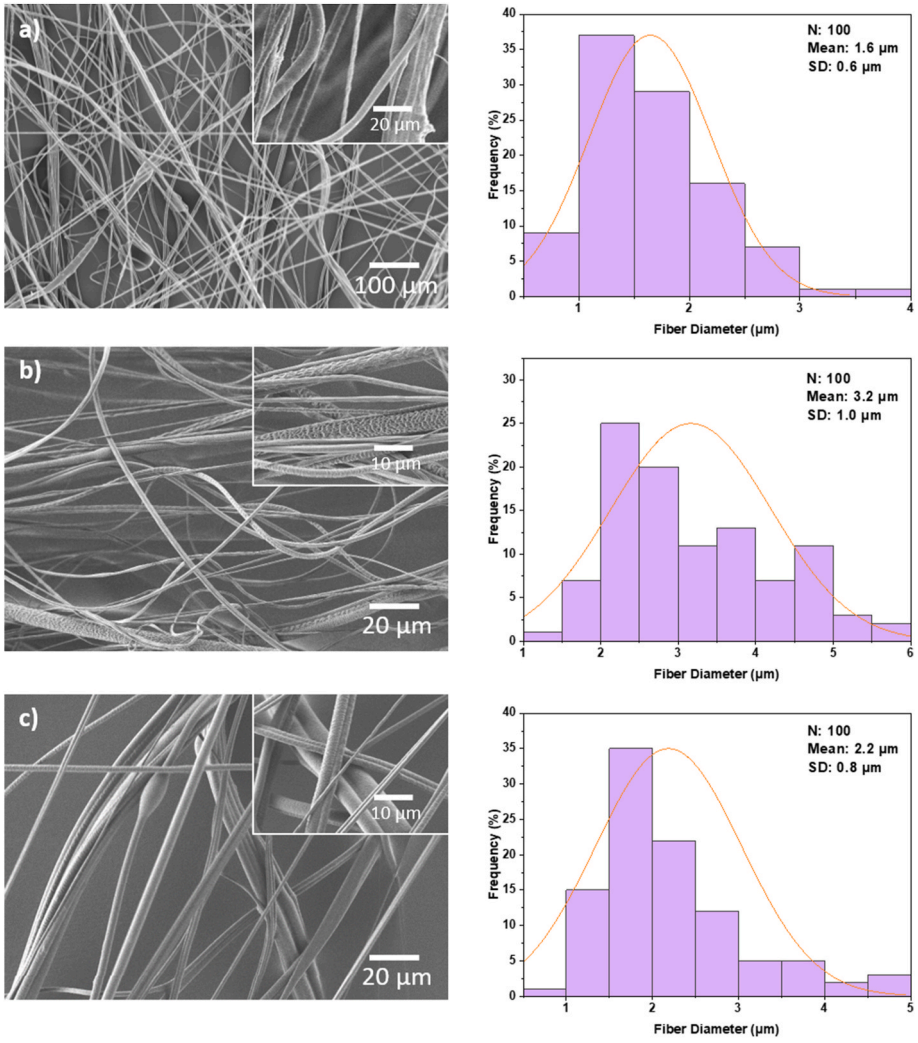

Fig. 8. SEM micrographs of IBP loaded fiber composites: a) 15 w/v % PEO 4 wt % IBP, b) 15 w/v % PCL 4 wt % IBP, and c) 4:1 PCL:PEO 4 wt % IBP, all spun at 10 000 rpm and 0.1 MPa applied pressure.

denotes a homogenous dispersion of IBP in the polymer solutions. The successful formation of continuous bead-free fibers with optimized (4:1) binary PCL:PEO-IBP (Fig. 8 (c)) achieved an average diameter of 2.2 µm and a PDI of 36 %. All three polymeric composites exhibit a monodisperse distribution. Although the average diameters of IBP-loaded fibers were smaller than those of non-loaded drug fibers, the link between IBP integration cannot be clearly established. Similar to the rheology results, this is explained by the incorporation of IBP occurring at a low concentration. The SEM micrographs do not show a significant difference in the morphology or topography of the composites, implying that the IBP was embedded in the polymer matrix.

3.6. Production rate

Scaling up other existing fiber manufacturing techniques, such as electrospinning, has been an ongoing challenge. To date, binary polymeric fibers have been produced in laboratory settings at a low production rate [49]. However, PG has proved to overcome this constraint. It facilitates the manufacture of fibers at substantially higher rates while retaining a more consistent and uniform fiber morphology by combining centrifugal force with controlled pressure. The production rates of PEO-IBP, PCL-IBP and PCL:PEO-IBP were analyzed. As shown in Fig. 9, PEO-IBP revealed a production rate of 17 g h^{-1} while PCL-IBP demonstrated a significantly higher yield of 45 g h^{-1}. However, PCL:PEO-IBP

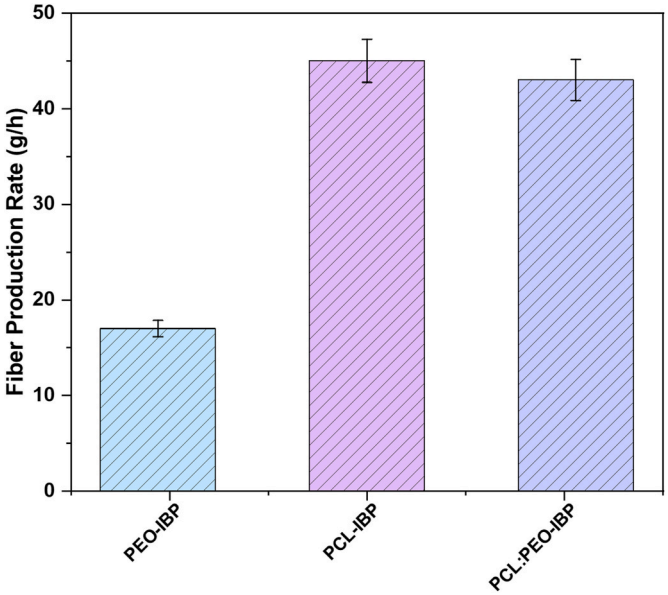

Fig. 9. Production rate of PEO-IBP, PCL-IBP and PCL:PEO-IBP composites produced by pressurized gyration.

displayed a slightly lower production rate of 43 g h^{-1} in comparison to PCL-IBP composites. This is due to the small incorporation of PEO to PCL in the binary system with a 4:1 ratio, resulting in a reduced fiber diameter. Variables such as solvent, polymer type, centrifugal force, and pressure often influence production rate outcomes. During the fabrication process for this study, the applied pressure, rotational speed, and solvent were all kept constant. Thus, the polymer molecular weight and ratios are the fundamental factors that can determine the difference in the generated fiber composites. Higher molecular weights often result in more viscous solutions, which may affect processing ease and fiber production. In this instance, PEO-IBP composites possessed a lower average diameter than PCL-IBP composites, indicating that the higher molecular weight of PEO may have resulted in finer fibers under the specified conditions. Furthermore, the average fiber diameter is proportional to the manufacturing rate. Finer fibers are often created at a higher rate since they require less material to form. The findings presented here endorse this general trend, as PEO-IBP composites exhibit the smallest diameter at 1.6 μm and the lowest production rate, whereas PCL-IBP fibers possess a larger diameter of 3.2 μm and a higher production rate. In contrast, the binary combination of PCL and PEO yields an intriguing outcome. The PCL:PEO average diameter of 2.2 μm falls between that of PCL-IBP and PEO-IBP fibers. This suggests that the combination of PCL and PEO may have an optimal balance of characteristics for this procedure, resulting in a production rate comparable to PCL-IBP composites.

3.7. Fourier-transform infrared (FTIR) spectral analysis

Chemical compositions of PEO, PCL, optimized PCL:PEO, IBP, PEO-IBP, PCL-IBP and PCL:PEO-IBP fibers were analyzed using FTIR (Fig. 10). FTIR spectrum for PEO fibers show an absorption at 2883 cm^{-1} corresponding to C–H stretching alkane group. Another peak was shown at 1466 cm^{-1} indicative of C–H bending alkane class, methylene group, followed by an O–H bending at 1342 cm^{-1}. PCL fibers show a strong absorption at 1722 cm^{-1} indicating C═O ester group stretch. Other prominent bands from this sample include two weak, broad peaks at 2863-2940 cm^{-1} corresponding to O–H stretching. All absorption peaks highlighted in the PEO and PCL composites were identified and highlighted in Fig. 10 for the binary PCL:PEO spectra. Furthermore, a strong C═O stretching band at 1709 cm^{-1} was detected in IBP, indicative of carboxylic acid followed by a O–H bending at 1342–1418 cm^{-1}. The PEO peaks displayed at 2883, 1466, and 1342 cm^{-1} were also detected in the PEO-IBP fiber spectra, followed by IBP absorption peak at 1066 cm^{-1}. Similarly, PCL peaks at 2940, 2863 and 1722 cm^{-1} were identified in the PCL-IBP fibers, as well as IBP peaks at 1418 and 1066 cm^{-1}. Lastly, PCL:PEO-IBP spectra detected absorption peaks of both PEO, and PCL fibers, as well as IBP. The FTIR spectra of PEO, PCL, binary PCL:PEO, and IBP loaded fibers were compared, and each spectrum denoted the presence of individual materials. It was demonstrated that PEO and PCL were successfully compounded and that there was no chemical interactions during the binary polymer system. Due to the absence of new chemical bonds, it can be assumed that the binary PCL:PEO polymer systems are immiscible. As a result, individual spectroscopy detected characteristics have remained consistent, and each fiber type has its own FTIR spectrum. This allows for material identification and differentiation.

3.8. Differential scanning calorimetry (DSC) analysis

The DSC analysis was performed to determine the thermal properties: glass transition (T_g), crystallization (T_c) and melting point (T_m) of the composites along with miscibility, and the presence of both polymers in the binary polymer system. To examine the thermal properties of all materials, a physical mix of PEO-IBP, PCL-IBP, and optimized PCL:PEO-IBP was utilized. Both PEO and PCL fiber composites exhibit a well-defined endothermic peak (Fig. 11). In relation to the PCL:PEO

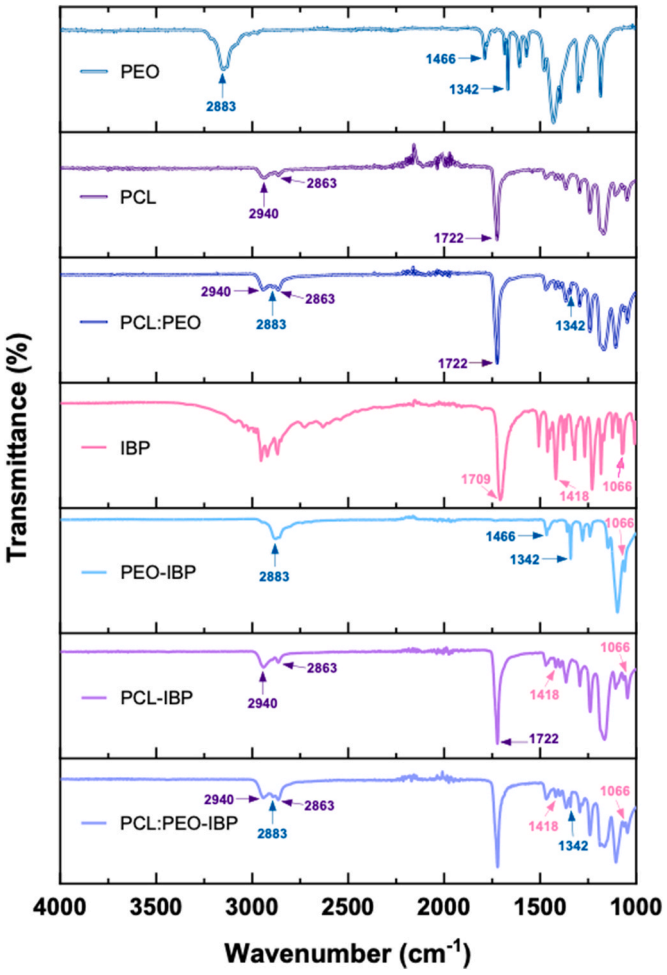

Fig. 10. FTIR spectra of PEO, PCL, PCL:PEO, IBP and IBP loaded singular/binary fibers.

(Fig. 11 (c)), the T_m of both polymers remain constant. PEO displayed a melting peak at 64 °C, while PCL demonstrated a melting peak at 59 °C. The occurrence of a broader and stretched peak in the binary polymer system is due to the integration of PEO. Further, the incorporation of IBP was detected in the binary polymer system, indicated at 155 °C, suggesting that the drug was molecularly dispersed within the polymer matrix. The appearance of distinct peaks in the DSC thermographs suggest that the binary polymer mixtures were immiscible. Given that PEO and PCL exhibit similar thermal properties [76], it would be difficult to determine if the binary polymer systems were miscible, and there is evidence from FTIR and SEM that suggest they are merely a physical blend.

3.9. In vitro release studies

3.9.1. Disintegration

The disintegration study demonstrates that PEO-IBP composites became wet instantly in 0.63 s and completely dissolved in 20.63 s (Fig. 12). The rapid wetting indicates the high-water affinity of these fibers, attributed to the hydrophilic nature of PEO within the composites. Hydrophilic materials have a strong tendency to absorb water quickly. Furthermore, the complete dissolution of the fibers implies that PEO is highly soluble in the testing medium (PBS), facilitating the release and absorption of IBP. Such characteristic can be advantageous for specific drug delivery applications, as it can lead to a quicker onset of therapeutic effects, particularly in pain management. Given the fast disintegration and dissolution properties, these composites can also be

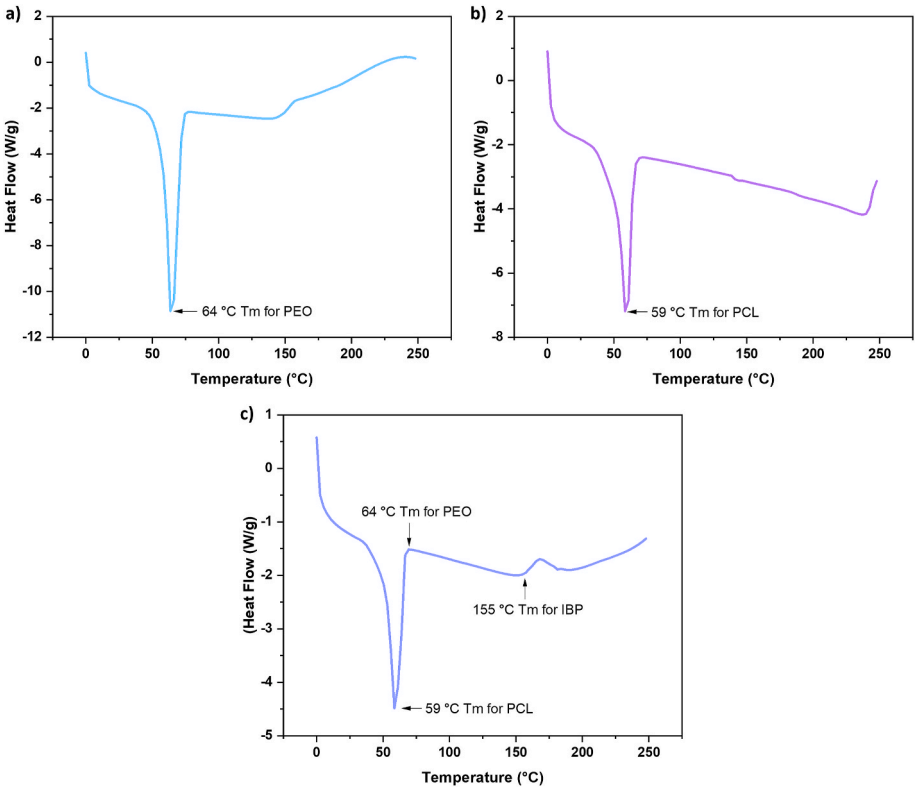

Fig. 11. DSC thermograms of a) PEO–IBP, b) PCL–IBP and c) PCL:PEO–IBP.

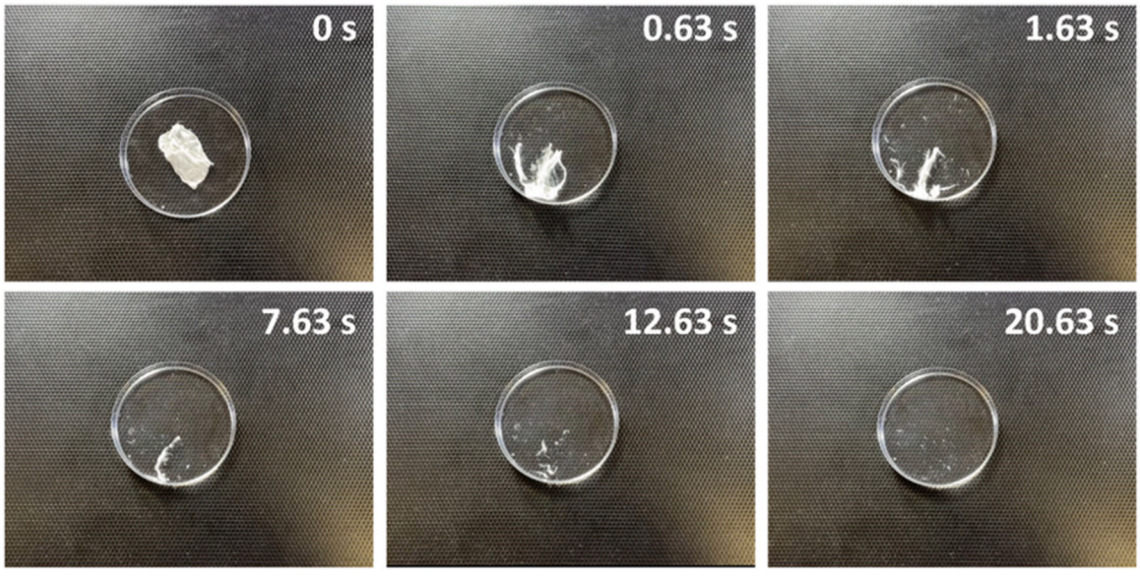

Fig. 12. Disintegration process of PEO-IBP composites at various time intervals throughout the disintegration study.

suitable for sublingual (under the tongue) and buccal (between the cheek and gums) drug delivery routes as solid unit dosage forms [77] such as tablets and capsules, and are considered promising alternatives to the traditional oral route for drug delivery [78]. For a drug to be administered sublingually, it must dissolve rapidly [79], a characteristic achievable with PEO fiber composites. Nevertheless, the sublingual and buccal routes may cause inconvenience for patients as they involve technical procedures to maintain the drug in the sublingual or buccal region for absorption without swallowing the drug. Not all drugs can be delivered in this manner and generally only small doses can be administered. Several physiological factors that may influence drug bioavailability, stability, efficacy, and safety should be considered in drug formulation design and development for effective absorption [78]. Furthermore, the drug must possess a balance of hydrophilic and lipophilic characteristics [80]. For the drug to bypass the epithelial barrier in these regions, it must be soluble in aqueous buccal fluids and should also have a high lipid solubility, which is usually accomplished by passive diffusion.

While the rapid wetting and dissolution properties of PEO-IBP composites provide numerous advantages for specific applications,

they impose limitations for other drug delivery systems, thereby making PEO composites undesirable on their own. The quick dissolution may result in a rapid release of IBP, leading to a short duration of action. Such behavior may not be desirable in situations requiring sustained drug release over an extended period of time. Patients may need to take numerous dosages more frequently, which is inconvenient. Furthermore, when a drug dissolves rapidly, it can be challenging to administer precise doses, especially for drugs with a narrow therapeutic window. This rapid dissolution may potentially pose stability challenges for certain drugs, especially those prone to degradation or hydrolysis in the presence of moisture. The high moisture absorption capacity of PEO can exacerbate these issues.

3.9.2. Dissolution

To investigate the release kinetics of IBP in different fiber matrices, an *in vitro* dissolution study of PEO-IBP, PCL-IBP, and PCL:PEO-IBP composites were performed. Fig. 13 (c) indicates that all three composites achieved a high encapsulation efficiency (EE) for IBP. PEO-IBP revealed a slightly higher EE profile (73 % ± 3.7) than PCL-IBP (70 %). However, when compared to PCL-IBP, PCL:PEO-IBP displayed a similar profile (73 % ± 3.5) to PEO-IBP. The presence of PEO and its hydrophilic nature in the binary polymer system can aid in enhanced encapsulation efficiency.

The PEO-IBP composite shows a rapid release profile, with complete release in less than 1 min (Fig. 13 (a)). In comparison to PEO-IBP composites, PCL-IBP fibers reveal a slower and more sustained drug release profile (Fig. 13 (b)). There was limited drug release during the initial 2 h, with only 14 % ± 0.003 release. Due to PCL's hydrophobicity, slow degradation rate, and resistance to water penetration, this lag phase was expected, thus the initial drug release was minimal. At 2–8 h, there was a steady and continuous rise in drug release, reaching 56 % ± 0.01. This phase exemplifies the controlled release capabilities of PCL; as the polymer degrades, the IBP diffuses out, resulting in a sustained profile. In addition, a significant amount of IBP was released between 8 and 72 h, with the release increasing from 56 % ± 0.01–87 % ± 0.003. The gradual biodegradation of PCL ensured that the IBP was released at a controlled rate over an extended period, making it appropriate for long-term therapeutic applications. The rate of drug release appeared to level off after 72 h, indicating a near-constant release rate. The cumulative release reached 87 % ± 0.003, implying that the drug could ultimately reach a plateau phase where further release is low. While PCL's hydrophobicity and slow degradation rate serve as an appropriate carrier for long-term sustained release applications, its lack of hydrophilicity makes it an unfavorable substrate for cell adhesion, proliferation, and wound dressings [81]. Moreover, PCL:PEO-IBP composites demonstrated a distinct profile; during the initial 8 h, a significant amount of IBP was released, reaching 85 % ± 0.0006. The presence of PEO in the binary polymer system was attributed to the rapid dissolution. PEO is recognized for its high-water solubility and rapid dissolution in aqueous conditions, which was also demonstrated for the PEO-IBP composites, resulting in immediate drug release. Moreover, there was a gradual and sustained increase in IBP release at 8–72 h, reaching 96 % ± 0.003. The sustained release phase was associated to the properties of PCL, which is less water-soluble with slow degradation rate. Additionally, PCL-IBP and PCL:PEO-IBP demonstrate comparable sustained release characteristics; however, PCL:PEO-IBP composites attain a higher cumulative release of 96.05 % ± 0.003 at 72 h as opposed to PCL-IBP composites with 87.44 % ± 0.003 at 72 h. But both PCL-IBP and PCL:PEO-IBP results can be attributed to a mechanism of simple diffusion. Similarly, Alimohammadi and co-workers [82] reported that the inclusion of PCL in a blend system is essential for sustained drug release for tissue engineering applications. They fabricated PCL/chitosan (CS)

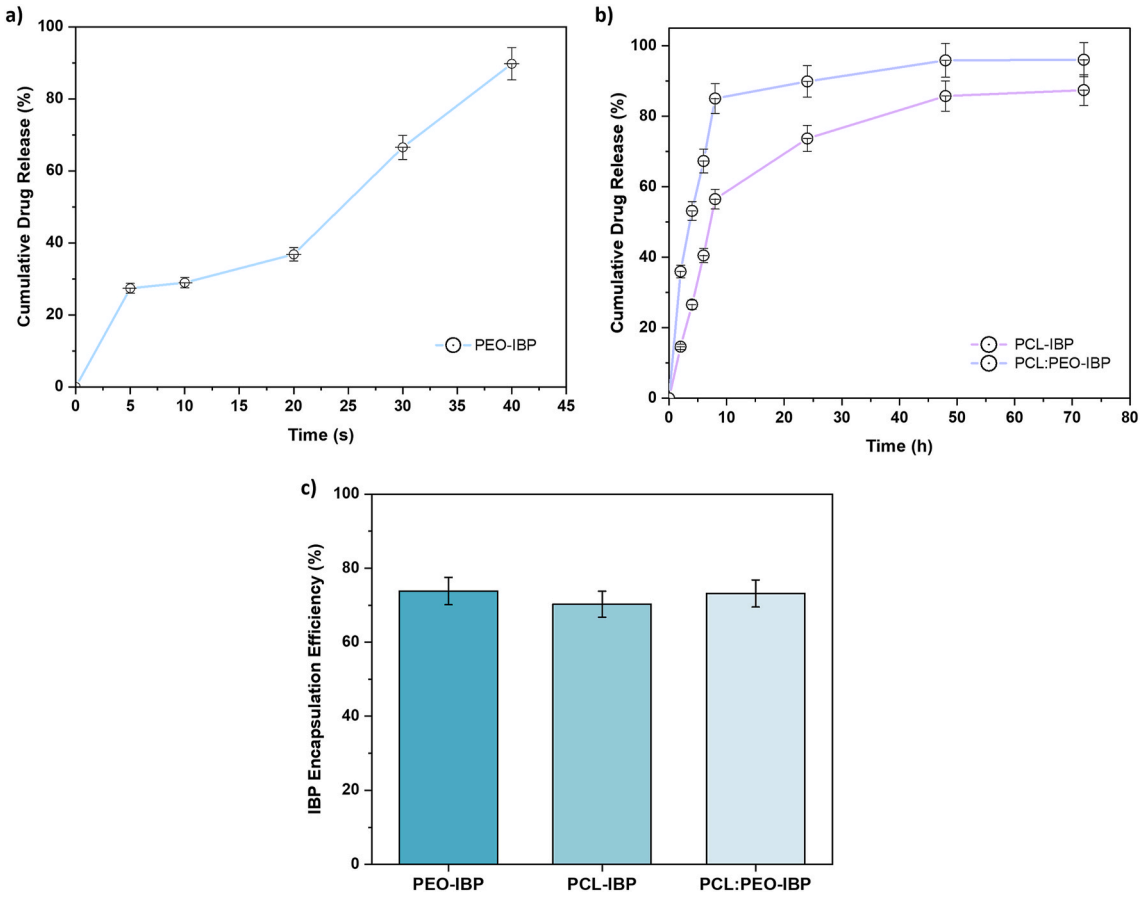

Fig. 13. a) IBP released from PEO fibers, b) IBP released from PCL and optimized binary PCL:PEO fibers and c) encapsulation efficiency of IBP in all three composites.

nanofibrous membranes and achieved a sustained release profile for more than 25 days for localized drug release applications with a high risk of infection and inflammation, such as post-surgery tendon adhesion, bone regeneration, and wound healing. Electrospun PCL/gelatin blend nanofibers were also fabricated by Xue et al. [83] that achieved sustained drug release over 20 days for guided bone regeneration membranes.

This binary polymer system exhibits the development of a modified material by combining the advantages of both PCL and PEO that offer a balanced release profile with an initial rapid release. Such versatility is advantageous for drug delivery systems that require both immediate therapeutic effect and long-term efficacy, for applications such as wound healing, pain management and anti-inflammation. In light of PEO's hydrophilicity, wound exudate can be collected while maintaining an adequately moist wound environment for cell adhesion and growth [84]. To reduce the bacterial population at wound sites, early drug release is required for wound healing. As a result, infection and inflammation will be eliminated. Due to the hydrophilic qualities incorporated in the binary polymer system, an initial rapid release is expected, followed by a sustained drug release as a result of PCL, which leads to a lower drug dosage over a prolonged period. An effective rate of wound healing is attributed to pain management and inflammation [85], which can be achieved with the binary polymer system, as it permits tailored drug release and a hydrophobic-hydrophilic balance by modifying polymer ratios. This strategy will provide rapid pain relief, followed by sustained release to maintain a baseline level of the drug. Similar findings were reported by Amiri et al. [86] with the blend system of CS-PEO nanofibers that achieved a sustained drug release of up to 12 days for local antibiotic delivery and wound healing. Cam et al. [87] also investigated the blend system of polyvinyl-pyrrolidone (PVP)/PCL fibers and obtained a sustained drug release over 14 days, attributed to the hydrophobic character of PCL for an effective treatment strategy of diabetic wound healing.

3.10. Mathematical modelling

For PEO the dissolution is assumed, as described by Eq. 8. Fitting this form to the experimental results gives $\tau = 69\ s$, with the result shown in Fig. 14 (a). A similar expression for release fraction $\varphi NWp(t) = t/\tau$ would apply to dissolution from one surface of a flat pellet, with the radius r_0 replaced by the initial pellet thickness h_0, and so it is useful to compare the results here with such an experiment [88] with pellets 2.5 mm thick, a factor of 3125 times the radius here. That would lead to a time constant of about 60 h, longer than the approximately 12 h that would be estimated for the pellets, but acceptable agreement given the differences in experimental conditions (for example, application of stirring or static release medium).

For PCL and PCL:PEO fibers the release is well described by the Fickian diffusion model, Eq. (7). The resulting fits are shown in Fig. 14 (b), and the diffusion coefficients that can be deduced are $1.3 \times 10^{13}\ m^2 s^{-1}$ for ibuprofen in PCL and $3.6 \times 10^{-14}\ m^2 s^{-1}$ in PCL:PEO.

4. Conclusions

In this study, the influence of various PCL:PEO polymer ratios on the morphologies of binary fibers were examined. The polymer characteristics, in particular the PEO ratio, were shown to be strongly correlated with viscosity, surface tension, fiber diameter and swelling behavior. In terms of uniformity and physical properties, PCL:PEO 4:1 was found to be an optimal binary polymer formulation for potential biomedical engineering applications. This binary polymer system can produce enhanced bead-free aligned fibers, adequate pore formation, and sufficient fiber swelling capabilities. Along with FTIR and DSC analyses, the presence of both polymers and incorporated IBP were investigated. Further, *in vitro* drug release studies confirmed the effectiveness of binary composites. The pattern of drug release from binary PCL:PEO fibers proved to be a compromise between PCL and PEO properties. The initial rapid release was governed by PEO's fast disintegration, followed by a continuous release phase, caused by PCL's controlled degradation. This mixture enabled a balanced and versatile release profile, or rapid therapeutic action and a steady, sustained release for long-term efficacy. Therefore, binary PCL:PEO composites would be favorable for drug delivery applications requiring both instant and long-term drug release. The work presented here demonstrates that PEO and PCL can successfully produce optimized binary polymer systems in different ratios to form various polymer morphological and physical properties, however, the choice of total polymer concentration, binary ratio, and solvent choice to blend the materials can lead to completely different outcomes.

CRediT authorship contribution statement

Ayda Afshar: Writing – review & editing, Writing – original draft, Visualization, Validation, Project administration, Methodology, Investigation, Formal analysis, Data curation, Conceptualization. **Hamta Majd:** Writing – review & editing, Visualization, Methodology, Investigation, Formal analysis, Data curation. **Anthony Harker:** Writing – review & editing, Supervision, Project administration, Conceptualization. **Mohan Edirisinghe:** Writing – review & editing, Supervision, Resources, Project administration, Funding acquisition, Conceptualization.

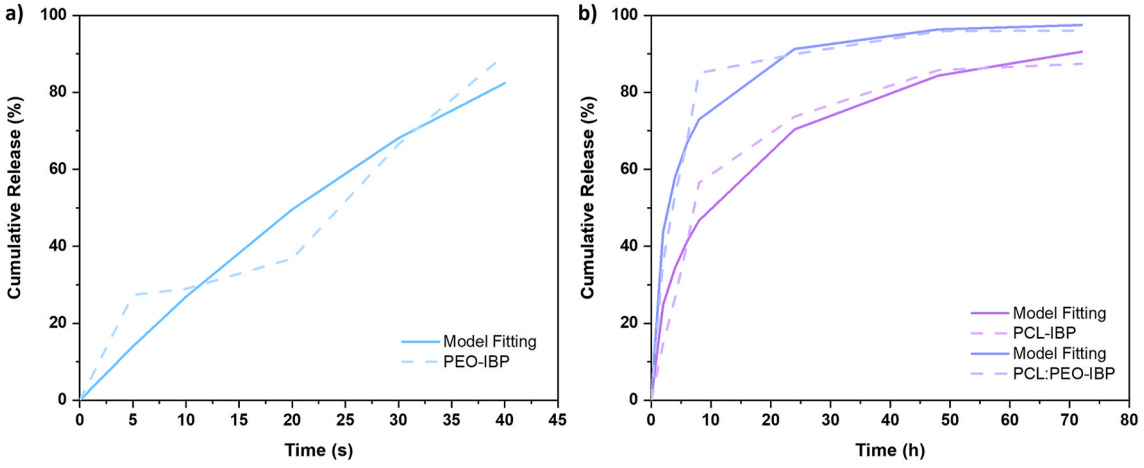

Fig. 14. a) Fit of simple dissolution model (dashed) for the PEO fibers loaded with IBP (solid) for the data and b) Fit of a diffusive release model (dashed) for PCL and PCL:PEO fibers loaded with IBP (solid) for the data.

Declaration of competing interest

The authors declare that they have no known competing financial interests or personal relationships that could have appeared to influence the work reported in this paper.

Data availability

Data will be made available on request.

Acknowledgement

Ayda Afshar would like to thank University College London for facilitating her doctoral research. UKRI is thanked for facilitating the setting up of pressurized gyration research at UCL (grants EP/S016872/1, EP/N034228/1, and EP/L023059/1).

References

[1] A.M. Al-Enizi, M.M. Zagho, A.A. Elzatahry, Polymer-based electrospun nanofibers for biomedical applications, Nanomaterials 8 (4) (2018).
[2] S. Columbus, D. Painuly, R.P. Nair, V.K. Krishnan, Role of PEGylated CdSe-ZnS quantum dots on structural and functional properties of electrospun polycaprolactone scaffolds for blood vessel tissue engineering, Eur. Polym. J. (2021) 151.
[3] A.K. Pearce, R.K. O'Reilly, Polymers for biomedical applications: the importance of hydrophobicity in directing biological interactions and application efficacy, Biomacromolecules 22 (11) (2021) 4459–4469.
[4] M.H. Farzaei, P. Derayat, Z. Pourmanouchehri, M. Kahrarian, Z. Samimi, M. Hajialyani, et al., Characterization and evaluation of antibacterial and wound healing activity of naringenin-loaded polyethylene glycol/polycaprolactone electrospun nanofibers, J. Drug Deliv. Sci. Technol. 81 (2023) 104182.
[5] G. Mann, P.M. Gurave, A. Kaul, K.G. Kadiyala, M. Pokhriyal, R.K. Srivastava, et al., Polymeric and electrospun patches for drug delivery through buccal route: formulation and biointerface evaluation, J. Drug Deliv. Sci. Technol. 68 (2022) 103030.
[6] S. Sagadevan, R. Schirhagl, M.Z. Rahman, M.F. Bin Ismail, J.A. Lett, I. Fatimah, et al., Recent advancements in polymer matrix nanocomposites for bone tissue engineering applications, J. Drug Deliv. Sci. Technol. 82 (2023) 104313.
[7] E. Mavrokefalou, P.K. Monou, D. Tzetzis, N. Bouropoulos, I.S. Vizirianakis, D. G. Fatouros, Preparation and in vitro evaluation of electrospun sodium alginate fiber films for wound healing applications, J. Drug Deliv. Sci. Technol. 81 (2023) 104298.
[8] T.A. Jeckson, Y.P. Neo, S.P. Sisinthy, J.B. Foo, H. Choudhury, B. Gorain, Formulation and characterisation of deferoxamine nanofiber as potential wound dressing for the treatment of diabetic foot ulcer, J. Drug Deliv. Sci. Technol. 66 (2021) 102751.
[9] O.C. Farokhzad, R. Langer, Impact of nanotechnology on drug delivery, ACS Nano 3 (1) (2009) 16–20.
[10] L. Zhang, F.X. Gu, J.M. Chan, A.Z. Wang, R.S. Langer, O.C. Farokhzad, Nanoparticles in medicine: therapeutic applications and developments, Clin. Pharmacol. Therapeut. 83 (5) (2008) 761–769.
[11] D. Peer, J.M. Karp, S. Hong, O.C. FaroKhzad, R. Margalit, R. Langer, Nanocarriers as an emerging platform for cancer therapy, Nat. Nanotechnol. 2 (12) (2007) 751–760.
[12] O.C. Farokhzad, R. Langer, Nanomedicine: developing smarter therapeutic and diagnostic modalities, Adv. Drug Deliv. Rev. 58 (14) (2006) 1456–1459.
[13] L.S. Nair, C.T. Laurencin, Biodegradable polymers as biomaterials, Prog. Polym. Sci. 32 (8–9) (2007) 762–798.
[14] B.L. Seal, T.C. Otero, A. Panitch, Polymeric biomaterials for tissue and organ regeneration, Mater. Sci. Eng. R Rep. 34 (4–5) (2001) 147–230.
[15] U. Hayat, A. Raza, M. Bilal, H.M.N. Iqbal, J.-Y. Wang, Biodegradable polymeric conduits: platform materials for guided nerve regeneration and vascular tissue engineering, J. Drug Deliv. Sci. Technol. 67 (2022) 103014.
[16] Albanese A, Tang PS, Chan WCW. The effect of nanoparticle size, shape, and surface chemistry on biological systems. In: Yarmush ML, editor. Annual Review of Biomedical Engineering, Vol vol. 14. Annual Review of Biomedical Engineering. 142012. p. 1-16.
[17] S.E.A. Gratton, P.A. Ropp, P.D. Pohlhaus, J.C. Luft, V.J. Madden, M.E. Napier, et al., The effect of particle design on cellular internalization pathways, Proc. Natl. Acad. Sci. U. S. A. 105 (33) (2008) 11613–11618.
[18] A. Banerjee, J.P. Qi, R. Gogoi, J. Wong, S. Mitragotri, Role of nanoparticle size, shape and surface chemistry in oral drug delivery, J. Contr. Release 238 (2016) 176–185.
[19] K.T. Shalumon, N.S. Binulal, M. Deepthy, R. Jayakumar, K. Manzoor, S.V. Nair, Preparation, characterization and cell attachment studies of electrospun multi-scale poly(caprolactone) fibrous scaffolds for tissue engineering, J. Macromol. Sci., Pure Appl. Chem. 48 (1) (2011) 21–30.
[20] E. Malikmammadov, T.E. Tanir, A. Kiziltay, V. Hasirci, N. Hasirci, PCL and PCL-based materials in biomedical applications, J. Biomater. Sci. Polym. Ed. 29 (7–9) (2018) 863–893.
[21] R. Boia, P.A.N. Dias, J.M. Martins, C. Galindo-Romero, I.D. Aires, M. Vidal-Sanz, et al., Porous poly(epsilon-caprolactone) implants: a novel strategy for efficient intraocular drug delivery, J. Contr. Release 316 (2019) 331–348.
[22] J. Hollander, N. Genina, H. Jukarainen, M. Khajeheian, A. Rosling, E. Makila, et al., Three-Dimensional printed PCL-based implantable prototypes of medical devices for controlled drug delivery, J. Pharmaceut. Sci. 105 (9) (2016) 2665–2676.
[23] K. Kundu, A. Afshar, D.R. Katti, M. Edirisinghe, K.S. Katti, Composite nanoclay-hydroxyapatite-polymer fiber scaffolds for bone tissue engineering manufactured using pressurized gyration, Compos. Sci. Technol. (2021) 202.
[24] K.R. Remya, J. Joseph, S. Mani, A. John, H.K. Varma, P. Ramesh, Nanohydroxyapatite incorporated electrospun polycaprolactone/polycaprolactone-polyethyleneglycol-polycaprolactone blend scaffold for bone tissue engineering applications, J. Biomed. Nanotechnol. 9 (9) (2013) 1483–1494.
[25] S. Gautam, A.K. Dinda, N.C. Mishra, Fabrication and characterization of PCL/gelatin composite nanofibrous scaffold for tissue engineering applications by electrospinning method, Mater Sci Eng C-Mater Biol Appl. 33 (3) (2013) 1228–1235.
[26] O.S. Manoukian, C. Marin, A. Ahmad, R. James, S.G. Kumbar (Eds.), Biodegradable Injectable Implants for Long-Term Delivery of Contraceptives and Other Therapeutics. 41st Annual Northeast Biomedical Engineering Conference (NEBEC), Ieee, 2015 Apr 17-19, p. NY2015. Troy.
[27] F. Chen, C.N. Lee, S.H. Teoh, Nanofibrous modification on ultra-thin poly(epsilon-caprolactone) membrane via electrospinning, Mater. Sci. Eng. C-Biomimetic Supramolecul. Syst. 27 (2) (2007) 325–332.
[28] Z. Mirzaei, S. Kordestani S, S. Kuth, D.W. Schubert, R. Detsch, J.A. Roether, et al., Preparation and characterization of electrospun blend fibrous polyethylene oxide: polycaprolactone scaffolds to promote cartilage regeneration, Adv. Eng. Mater. 22 (9) (2020) 2000131.
[29] N. Recek, M. Resnik, H. Motaln, T. Lah-Turnsek, R. Augustine, N. Kalarikkal, et al., Cell adhesion on polycaprolactone modified by plasma treatment, Int. J. Polymer Sci. 2016 (2016) 9.
[30] J.K. Fink, Handbook of Engineering and Specialty Thermoplastics, Volume 2: Water Soluble Polymers, John Wiley & Sons, 2011.
[31] Y.J. Xu, L.M. Zou, H.W. Lu, Y.Z. Wei, J.B. Hua, S.Y. Chen, Preparation and characterization of electrospun PHBV/PEO mats: the role of solvent and PEO component, J. Mater. Sci. 51 (12) (2016) 5695–5711.
[32] Y.F. Li, H. Gregersen, J.V. Nygaard, W.L. Cheng, Y. Yu, Y.D. Huang, et al., Ultraporous nanofeatured PCL-PEO microfibrous scaffolds enhance cell infiltration, colonization and myofibroblastic differentiation, Nanoscale 7 (36) (2015) 14989–14995.
[33] M. Ebrahimifar, M. Taherimehr, Evaluation of in-vitro drug release of polyvinylcyclohexane carbonate as a CO2-derived degradable polymer blended with PLA and PCL as drug carriers, J. Drug Deliv. Sci. Technol. 63 (2021) 102491.
[34] M. Kaur, A. Sharma, V. Puri, G. Aggarwal, P. Maman, K. Huanbutta, et al., Chitosan-based polymer blends for drug delivery systems, Polymers 15 (9) (2023).
[35] B. Darbasizadeh, S.A. Mortazavi, F. Kobarfard, M.R. Jaafari, A. Hashemi, H. Farhadnejad, et al., Electrospun Doxorubicin-loaded PEO/PCL core/sheath nanofibers for chemopreventive action against breast cancer cells, J. Drug Deliv. Sci. Technol. 64 (2021) 102576.
[36] H.W. Toh, D.W.Y. Toong, J.C.K. Ng, V. Ow, S. Lu, L.P. Tan, et al., Polymer blends and polymer composites for cardiovascular implants, Eur. Polym. J. 146 (2021) 110249.
[37] S. Madhumanchi, T. Srichana, A. Domb, Polymeric Biomaterials, 2021, pp. 49–100.
[38] H.M. Zhang, M. Zuo, X.Y. Zhang, X.Y. Shi, L. Yang, S.H. Sun, et al., Effect of agglomeration on the selective distribution of nanoparticles in binary polymer blends, Compos. Appl. Sci. Manuf. 149 (2021) 6.
[39] M.E. Hoque, W.Y. San, F. Wei, S.M. Li, M.H. Huang, M. Vert, et al., Processing of polycaprolactone and polycaprolactone-based copolymers into 3D scaffolds, and their cellular responses, Tissue Eng. 15 (10) (2009) 3013–3024.
[40] T.H. Nguyen, B.T. Lee, Electro-spinning of PLGA/PCL blends for tissue engineering and their biocompatibility, J. Mater. Sci. Mater. Med. 21 (6) (2010) 1969–1978.
[41] L. Yu, K. Dean, L. Li, Polymer blends and composites from renewable resources, Prog. Polym. Sci. 31 (6) (2006) 576–602.
[42] D.M. García Cruz, D.F. Coutinho, J.F. Mano, J.L. Gómez Ribelles, M. Salmerón Sánchez, Physical interactions in macroporous scaffolds based on poly (ε-caprolactone)/chitosan semi-interpenetrating polymer networks, Polymer 50 (9) (2009) 2058–2064.
[43] G. Kim, J. Park, S. Park, Surface-treated and multilayered poly(ε-caprolactone) nanofiber webs exhibiting enhanced hydrophilicity, J. Polym. Sci. B Polym. Phys. 45 (15) (2007) 2038–2045.
[44] F. Xu, F.Z. Cui, Y.P. Jiao, Q.Y. Meng, X.P. Wang, X.Y. Cui, Improvement of cytocompatibility of electrospinning PLLA microfibers by blending PVP, J. Mater. Sci. Mater. Med. 20 (6) (2009) 1331–1338.
[45] M.P. Prabhakaran, J.R. Venugopal, T. Ter Chyan, L.B. Hai, C.K. Chan, A.Y. Lim, et al., Electrospun biocomposite nanofibrous scaffolds for neural tissue engineering, Tissue Eng. 14 (11) (2008) 1787–1797.
[46] K.R. Remya, S. Chandran, S. Mani, A. John, P. Ramesh, Hybrid polycaprolactone/polyethylene oxide scaffolds with tunable fiber surface morphology, improved hydrophilicity and biodegradability for bone tissue engineering applications, J. Biomater. Sci. Polym. Ed. 29 (12) (2018) 1444–1462.
[47] N.E. Zander, J.A. Orlicki, A.M. Rawlett, T.P. Beebe, Electrospun polycaprolactone scaffolds with tailored porosity using two approaches for enhanced cellular infiltration, J. Mater. Sci. Mater. Med. 24 (1) (2013) 179–187.

[48] Ş.M. Eskitoros-Togay, Y.E. Bulbul, S. Tort, F. Demirtaş Korkmaz, F. Acartürk, N. Dilsiz, Fabrication of doxycycline-loaded electrospun PCL/PEO membranes for a potential drug delivery system, Int. J. Pharm. 565 (2019) 83–94.
[49] A. Afshar, M. Gultekinoglu, M. Edirisinghe, Binary polymer systems for biomedical applications, Int. Mater. Rev. (2022) 1–41.
[50] S. Meraz-Davila, C.E. Perez-Garcia, A.A. Feregrino-Perez, Challenges and advantages of electrospun nanofibers in agriculture: a review, Mater. Res. Express 8 (4) (2021).
[51] M. Acosta, V.L. Wiesner, C.J. Martinez, R.W. Trice, J.P. Youngblood, Effect of polyvinylpyrrolidone additions on the rheology of aqueous, highly loaded alumina suspensions, J. Am. Ceram. Soc. 96 (5) (2013) 1372–1382.
[52] Z.-C. Yao, J.-C. Wang, Z. Ahmad, J.-S. Li, M.-W. Chang, Fabrication of patterned three-dimensional micron scaled core-sheath architectures for drug patches, Mater. Sci. Eng. C 97 (2019) 776–783.
[53] A.A. Noyes, W.R. Whitney, The rate of solution of solid substances in their OWN solutions, J. Am. Chem. Soc. 19 (12) (1897) 930–934.
[54] M. Eltayeb, E. Stride, M. Edirisinghe, A. Harker, Electrosprayed nanoparticle delivery system for controlled release, Mater. Sci. Eng., C 66 (2016) 138–146.
[55] Y. Dai, J. Ahmed, M. Edirisinghe, Pressurized gyration: fundamentals, advancements, and future, Macromol. Mater. Eng. 308 (7) (2023) 2300033.
[56] X.Z. Hong, M. Edirisinghe, S. Mahalingam, Beads, beaded-fibres and fibres: tailoring the morphology of poly(caprolactone) using pressurised gyration, Mater Sci Eng C-Mater Biol Appl. 69 (2016) 1373–1382.
[57] C.L. Casper, J.S. Stephens, N.G. Tassi, D.B. Chase, J.F. Rabolt, Controlling surface morphology of electrospun polystyrene fibers: effect of humidity and molecular weight in the electrospinning process, Macromolecules 37 (2) (2003) 573–578.
[58] P. Gupta, C. Elkins, T.E. Long, G.L. Wilkes, Electrospinning of linear homopolymers of poly(methyl methacrylate): exploring relationships between fiber formation, viscosity, molecular weight and concentration in a good solvent, Polymer 46 (13) (2005) 4799–4810.
[59] M.R. Badrossamay, H.A. McIlwee, J.A. Goss, K.K. Parker, Nanofiber assembly by rotary jet-spinning, Nano Lett. 10 (6) (2010) 2257–2261.
[60] S. Mahalingam, M. Edirisinghe, Forming of polymer nanofibers by a pressurised gyration process, Macromol. Rapid Commun. 34 (14) (2013) 1134–1139.
[61] S. Shojaee, P. Emami, A. Mahmood, Y. Rowaiye, A. Dukulay, W. Kaialy, et al., An investigation on the effect of polyethylene oxide concentration and particle size in modulating theophylline release from tablet matrices, AAPS PharmSciTech 16 (6) (2015) 1281–1289.
[62] M. Cowman, T. Schmidt, P. Raghavan, A. Stecco, Viscoelastic properties of hyaluronan in physiological conditions, F1000Research 4 (2015).
[63] K.N. Clayton, J.W. Salameh, S.T. Wereley, T.L. Kinzer-Ursem, Physical characterization of nanoparticle size and surface modification using particle scattering diffusometry, Biomicrofluidics 10 (5) (2016).
[64] J.M. Hughes, P.M. Budd, A. Grieve, P. Dutta, K. Tiede, J. Lewis, Highly monodisperse, lanthanide-containing polystyrene nanoparticles as potential standard reference materials for environmental "nano" fate analysis, J. Appl. Polym. Sci. 132 (24) (2015).
[65] M. Danaei, M. Dehghankhold, S. Ataei, F.H. Davarani, R. Javanmard, A. Dokhani, et al., Impact of particle size and polydispersity index on the clinical applications of lipidic nanocarrier systems, Pharmaceutics 10 (2) (2018).
[66] X. Hong, M. Edirisinghe, S. Mahalingam, Beads, beaded-fibres and fibres: tailoring the morphology of poly (caprolactone) using pressurised gyration, Mater. Sci. Eng. C 69 (2016) 1373–1382.
[67] H. Wee, B.W. Wagoner, P.M. Kamat, O.A. Basaran, Effects of surface viscosity on breakup of viscous threads, Phys. Rev. Lett. 124 (20) (2020).
[68] D. Jeyachandran, M. Cerruti, Glass, ceramic, polymeric, and composite scaffolds with multiscale porosity for bone tissue engineering, Adv. Eng. Mater. 25 (17) (2023) 2201743.
[69] J. Mu, D. Luo, W. Li, Y. Ding, Multiscale polymeric fibers for drug delivery and tissue engineering, Biomed. Tech. 5 (2024) 60–72.
[70] S. Hulsey, S. Absar, H. Choi (Eds.), Comparative Study of Polymer Dissolution Techniques for Electrospinning. 45th SME North American Manufacturing Research Conference (NAMRC), Univ Southern California, Los Angeles, 2017 Jun 04-08, p. CA2017.
[71] H. Chen, X.H. Chen, H.Y. Chen, X. Liu, J.X. Li, J. Luo, et al., Molecular interaction, chain conformation, and rheological modification during electrospinning of hyaluronic acid aqueous solution, Membranes 10 (9) (2020).
[72] L.L. Ma, L. Deng, J.M. Chen, Applications of poly(ethylene oxide) in controlled release tablet systems: a review, Drug Dev. Ind. Pharm. 40 (7) (2014) 845–851.
[73] D. Husken, R.J. Gaymans, The structure of water in PEO-based segmented block copolymers and its effect on transition temperatures, Macromol. Chem. Phys. 209 (9) (2008) 967–979.
[74] G. Zidan, C. Ann Greene, A. Seyfoddin, 2 - formulation design in drug delivery, in: A. Seyfoddin, S.M. Dezfooli, C.A. Greene (Eds.), Engineering Drug Delivery Systems, Woodhead Publishing, 2020, pp. 17–41.
[75] Z. Wei, E. Liu, H. Li, Z. Wei, Z. lv, Release characteristics of different diameter ultrafine fibers as antibacterial materials, J. Innov. Optic. Health Sci. 14 (2) (2021) 2041005.
[76] M. Dalton, F. Ebrahimi, H. Xu, K. Gong, G. Fehrenbach, E. Fuenmayor, et al., The influence of the molecular weight of poly(ethylene oxide) on the hydrolytic degradation and physical properties of polycaprolactone binary blends, Macromol 3 (3) (2023) 431–450.
[77] S. Adepu, S. Ramakrishna, Controlled drug delivery systems: current status and future directions, Molecules 26 (19) (2021).
[78] S. Hua, Advances in nanoparticulate drug delivery approaches for sublingual and buccal administration, Front. Pharmacol. 10 (2019) 1328.
[79] M. Kester, K.D. Karpa, K.E. Vrana, 1 - pharmacokinetics, in: M. Kester, K.D. Karpa, K.E. Vrana (Eds.), Elsevier's Integrated Review Pharmacology, second ed., W.B. Saunders, Philadelphia, 2012, pp. 1–15. Second Edition.
[80] L.L. Brunton, B.A. Chabner, B.C. Knollmann, Goodman & Gilman: Las bases farmacológicas de la terapéutica, McGraw hill, 2019.
[81] X. Chen, Q. Zhang, Y. Wang, J. Meng, M. Wu, H. Xu, et al., Fabrication and characterization of electrospun poly(caprolactone)/tannic acid scaffold as an antibacterial wound dressing, Polymers 15 (3) (2023).
[82] M. Alimohammadi, O. Fakhraei, A. Moradi, M. Kabiri, A. Moradi, M. Passandideh-Fard, et al., Controlled release of azithromycin from polycaprolactone/chitosan nanofibrous membranes, J. Drug Deliv. Sci. Technol. 71 (2022) 103246.
[83] J. Xue, Y. Niu, M. Gong, R. Shi, D. Chen, L. Zhang, et al., Electrospun microfiber membranes embedded with drug-loaded clay nanotubes for sustained antimicrobial protection, ACS Nano 9 (2) (2015) 1600–1612.
[84] J. Dulnik, D. Kołbuk, P. Denis, P. Sajkiewicz, The effect of a solvent on cellular response to PCL/gelatin and PCL/collagen electrospun nanofibres, Eur. Polym. J. 104 (2018) 147–156.
[85] V.U. Godakanda, H. Li, L. Alquezar, L. Zhao, L.-M. Zhu, R. de Silva, et al., Tunable drug release from blend poly(vinyl pyrrolidone)-ethyl cellulose nanofibers, Int. J. Pharm. 562 (2019) 172–179.
[86] N. Amiri, S. Ajami, A. Shahroodi, N. Jannatabadi, S. Amiri Darban, B.S. Fazly Bazzaz, et al., Teicoplanin-loaded chitosan-PEO nanofibers for local antibiotic delivery and wound healing, Int. J. Biol. Macromol. 162 (2020) 645–656.
[87] M.E. Cam, S. Yildiz, H. Alenezi, S. Cesur, G.S. Ozcan, G. Erdemir, et al., Evaluation of burst release and sustained release of pioglitazone-loaded fibrous mats on diabetic wound healing: an in vitro and in vivo comparison study, J. R. Soc. Interface 17 (162) (2020) 20190712.
[88] A. Körner, A. Larsson, Å. Andersson, L. Piculell, Swelling and polymer erosion for poly(ethylene oxide) tablets of different molecular weights polydispersities, J. Pharmaceut. Sci. 99 (3) (2010) 1225–1238.